



# HHS Public Access

Author manuscript

*Annu Rev Virol.* Author manuscript; available in PMC 2017 June 05.

Published in final edited form as:

*Annu Rev Virol.* 2016 September 29; 3(1): 237–261. doi:10.1146/annurev-virology-110615-042301.

## Structure, Function, and Evolution of Coronavirus Spike Proteins

Fang Li

Department of Pharmacology, University of Minnesota Medical School, Minneapolis, Minnesota 55455

### Abstract

The coronavirus spike protein is a multifunctional molecular machine that mediates coronavirus entry into host cells. It first binds to a receptor on the host cell surface through its S1 subunit and then fuses viral and host membranes through its S2 subunit. Two domains in S1 from different coronaviruses recognize a variety of host receptors, leading to viral attachment. The spike protein exists in two structurally distinct conformations, prefusion and postfusion. The transition from prefusion to postfusion conformation of the spike protein must be triggered, leading to membrane fusion. This article reviews current knowledge about the structures and functions of coronavirus spike proteins, illustrating how the two S1 domains recognize different receptors and how the spike proteins are regulated to undergo conformational transitions. I further discuss the evolution of these two critical functions of coronavirus spike proteins, receptor recognition and membrane fusion, in the context of the corresponding functions from other viruses and host cells.

### Keywords

coronavirus spike protein; prefusion conformation; postfusion conformation; receptor binding; membrane fusion; virus origin; virus evolution

### INTRODUCTION

Coronaviruses pose serious health threats to humans and other animals. From 2002 to 2003, severe acute respiratory syndrome coronavirus (SARS-CoV) infected 8,000 people, with a fatality rate of ~10% (1–4). Since 2012, Middle East respiratory syndrome coronavirus (MERS-CoV) has infected more than 1,700 people, with a fatality rate of ~36% (5, 6). Since 2013, porcine epidemic diarrhea coronavirus (PEDV) has swept throughout the United States, causing an almost 100% fatality rate in piglets and wiping out more than 10% of America's pig population in less than a year (7–9). In general, coronaviruses cause widespread respiratory, gastrointestinal, and central nervous system diseases in humans and other animals, threatening human health and causing economic loss (10, 11). Coronaviruses are capable of adapting to new environments through mutation and recombination with relative ease and hence are programmed to alter host range and tissue tropism efficiently

### DISCLOSURE STATEMENT

The author is not aware of any affiliations, memberships, funding, or financial holdings that might be perceived as affecting the objectivity of this review.

(12–14). Therefore, health threats from coronaviruses are constant and long-term. Understanding the virology of coronaviruses and controlling their spread have important implications for global health and economic stability.

Coronaviruses belong to the family *Coronaviridae* in the order *Nidovirales* (10, 11). They can be classified into four genera: *Alphacoronavirus*, *Betacoronavirus*, *Gammacoronavirus*, and *Deltacoronavirus* (Figure 1a). Among them, alpha- and betacoronaviruses infect mammals, gammacoronaviruses infect avian species, and deltacoronaviruses infect both mammalian and avian species. Representative alphacoronaviruses include human coronavirus NL63 (HCoV-NL63), porcine transmissible gastroenteritis coronavirus (TGEV), PEDV, and porcine respiratory coronavirus (PRCV). Representative betacoronaviruses include SARS-CoV, MERS-CoV, bat coronavirus HKU4, mouse hepatitis coronavirus (MHV), bovine coronavirus (BCoV), and human coronavirus OC43. Representative gamma- and deltacoronaviruses include avian infectious bronchitis coronavirus (IBV) and porcine deltacoronavirus (PdCV), respectively. Coronaviruses are large, enveloped, positive-stranded RNA viruses. They have the largest genome among all RNA viruses, typically ranging from 27 to 32 kb. The genome is packed inside a helical capsid formed by the nucleocapsid protein (N) and further surrounded by an envelope. Associated with the viral envelope are at least three structural proteins: The membrane protein (M) and the envelope protein (E) are involved in virus assembly, whereas the spike protein (S) mediates virus entry into host cells. Some coronaviruses also encode an envelope-associated hemagglutinin-esterase protein (HE). Among these structural proteins, the spike forms large protrusions from the virus surface, giving coronaviruses the appearance of having crowns (hence their name; *corona* in Latin means crown) (Figures 1b and 2a). In addition to mediating virus entry, the spike is a critical determinant of viral host range and tissue tropism and a major inducer of host immune responses.

The coronavirus spike contains three segments: a large ectodomain, a single-pass transmembrane anchor, and a short intracellular tail (Figure 1b,c). The ectodomain consists of a receptor-binding subunit S1 and a membrane-fusion subunit S2. Electron microscopy studies revealed that the spike is a clove-shaped trimer with three S1 heads and a trimeric S2 stalk (15–18) (Figures 1b and 2a). During virus entry, S1 binds to a receptor on the host cell surface for viral attachment, and S2 fuses the host and viral membranes, allowing viral genomes to enter host cells. Receptor binding and membrane fusion are the initial and critical steps in the coronavirus infection cycle; they also serve as primary targets for human interventions. In this article, I review the structure and function of coronavirus spikes and discuss their evolution.

## RECEPTOR RECOGNITION BY CORONAVIRUS SPIKE PROTEINS

Coronaviruses demonstrate a complex pattern for receptor recognition (19) (Figure 1d). For example, the alphacoronavirus HCoV-NL63 and the betacoronavirus SARS-CoV both recognize a zinc peptidase angiotensin-converting enzyme 2 (ACE2) (20, 21). Moreover, HCoV-NL63 and other alphacoronaviruses recognize different receptors: other alphacoronaviruses such as TGEV, PEDV, and PRCV recognize another zinc peptidase, aminopeptidase N (APN) (22–25). Similarly, SARS-CoV and other betacoronaviruses

recognize different receptors: MERS-CoV and HKU4 recognize a serine peptidase, dipeptidyl peptidase 4 (DPP4) (26, 27); MHV recognizes a cell adhesion molecule, carcinoembryonic antigen-related cell adhesion molecule 1 (CEACAM1) (28, 29); BCoV and OC43 recognize sugar (30). The alphacoronaviruses TGEV and PEDV and the gammacoronavirus IBV also use sugar as receptors or coreceptors (23, 31–34). Other than their role in viral attachment, these coronavirus receptors have their own physiological functions (35–41). The diversity of receptor usage is an outstanding feature of coronaviruses. To further compound the complexity of the issue, the S1 subunits from different genera share little sequence similarity, whereas those from the same genus have significant sequence similarity (42). Therefore, the following questions have been raised regarding receptor recognition by coronaviruses: (a) How do coronaviruses from different genera recognize the same receptor protein? (b) How do coronaviruses from the same genus recognize different receptor proteins? (c) What is the molecular basis for coronavirus spikes to recognize sugar receptors and function as viral lectins?

Two major domains in coronavirus S1, N-terminal domain (S1-NTD) and C-terminal domain (S1-CTD), have been identified (Figure 1c,d). One or both of these S1 domains potentially bind receptors and function as the receptor-binding domain (RBD). S1-NTDs are responsible for binding sugar (23, 34, 43, 44), with the only known exception being betacoronavirus MHV S1-NTD that recognizes a protein receptor CEACAM1 (45). S1-CTDs are responsible for recognizing protein receptors ACE2, APN, and DPP4 (23, 46–51). Crystal structures have been determined for a number of S1 domains complexed with their respective receptor (Figure 1d). These structures, along with functional studies, have addressed many of the puzzles surrounding receptor recognition by coronaviruses.

## RECEPTOR RECOGNITION BY CORONAVIRUS S1-CTDS

The structure of betacoronavirus SARS-CoV S1-CTD complexed with human ACE2 provided the first atomic view of coronavirus S1 (52, 53) (Figure 3a). SARS-CoV S1-CTD contains two subdomains: a core structure and a receptor-binding motif (RBM). The core structure is a five-stranded antiparallel  $\beta$ -sheet. The RBM presents a gently concave outer surface to bind ACE2. The base of this concave surface is a short, two-stranded antiparallel  $\beta$ -sheet, and two ridges are formed by loops. The ectodomain of ACE2 contains a membrane-distal peptidase domain and a membrane-proximal collectrin domain (54). Several virus-binding motifs (VBMs) have been identified on the outer surface of the peptidase domain, away from the buried peptidase catalytic site (52). SARS-CoV binding does not interfere with the enzymatic activity of ACE2, nor does the enzymatic activity of ACE2 play any role in SARS-CoV entry (55).

Research on SARS-CoV-ACE2 interactions has provided novel insight into cross-species transmissions of SARS-CoV. During the SARS epidemic, highly similar SARS-CoV strains were isolated from both human patients and palm civets from nearby animal markets (56). Their S1-CTDs differ by only two residues in the RBM region: Asn479 and Thr487 in human viral strains become Lys479 and Ser487 in civet viral strains, respectively (Figure 3b,c). However, human SARS-CoV S1-CTD binds to human ACE2 much more tightly than civet SARS-CoV S1-CTD does. Two virus-binding hot spots have been identified on human

ACE2, centering on ACE2 residues Lys31 and Lys353, respectively (57–59) (Figure 3b). Both hot spots consist of a salt bridge buried in a hydrophobic environment and contribute critically to virus-receptor binding. Residues 479 and 487 in SARS-CoV S1-CTD interact closely with these hot spots and are under selective pressure to mutate. Two naturally selected viral mutations, K479N and S487T, strengthened the hot spot structures and enhanced the binding affinity of S1-CTD for human ACE2 (55, 57–59) (Figure 3c). Consequently, these two mutations played important roles in the civet-to-human and human-to-human transmissions of SARS-CoV during the SARS epidemic (13, 55, 57–61). Compared to human ACE2, rat ACE2 contains two different residues that disfavor SARS-CoV binding: His353 disturbs the hot spot structure centering on Lys353, whereas Asn82 introduces an *N*-linked glycan, presenting steric interference with SARS-CoV binding (52) (Figure 3d). Mouse ACE2 also contains His353 but does not have the *N*-linked glycan at the 82 position. Thus, rat ACE2 is not a receptor for SARS-CoV, whereas mouse ACE2 is a poor receptor. Consequently, SARS-CoV does not infect rat cells, and it infects mouse cells inefficiently (62, 63). SARS-like coronaviruses (SLCoVs) have been identified in bats, and some can infect human cells (64–68). Structural details on how these bat SLCoV S1-CTDs interact with ACE2 from different mammalian species still wait to be determined. Overall, these studies on SARS-CoV-ACE2 interactions reveal that (a) one or a few mutations in viral RBDs can cause serious epidemic outcomes and (b) one or a few residue variations in receptor homologs from different animal species can form critical barriers for cross-species transmissions of viruses.

The structure of betacoronavirus MERS-CoV S1-CTD complexed with human DPP4, when compared with SARS-CoV, presented an interesting example of how two structurally similar viral RBDs recognize different protein receptors (Figure 3a,e). Like SARS-CoV S1-CTD, MERS-CoV S1-CTD also contains two subdomains, a core structure and an RBM (69–71). The core structures of MERS-CoV and SARS-CoV S1-CTDs are similar to each other, whereas their RBMs are markedly different. In contrast to the loop-dominated and gently concave surface of SARS-CoV RBM, MERS-CoV RBM consists of a four-stranded antiparallel  $\beta$ -sheet, presenting a relatively flat surface to bind DPP4. On the other hand, DPP4 forms a homodimer and each monomer contains a hydrolase domain and a  $\beta$ -propeller domain (72). The VBMs are located on the outer surface of the  $\beta$ -propeller domain, away from the peptidase catalytic site. The variations of VBM residues on DPP4 homologs from different mammalian species pose a barrier for cross-species transmissions of MERS-CoV. For example, mouse and rat DPP4 molecules are both poor receptors for MERS-CoV because they each contain a number of VBM residues that disfavor MERS-CoV binding (73–75). Camel DPP4 is an effective receptor for MERS-CoV due to its conserved VBM residues (76). Indeed, MERS-CoV has been isolated from camels, suggesting a camel-to-human transmission of MERS-CoV (77, 78). Several MERS-related coronaviruses have been isolated from bats (79–81). Among them, HKU4 recognizes DPP4 using a structural mechanism similar to that used by MERS-CoV, indicating a bat origin of MERS-CoV (27, 82). Overall, these studies reveal that viral RBDs with a conserved core structure can recognize different receptors through structural variations in their RBM, and they also reinforce the concept that receptor recognition is a critical determinant of viral host ranges.

The structure of alphacoronavirus HCoV-NL63 S1-CTD complexed with human ACE2, when compared with SARS-CoV, showed how two structurally divergent viral RBDs recognize the same protein receptor (83) (Figures 3a and 4a). HCoV-NL63 S1-CTD contains a core structure and three RBM loops. The core structure of HCoV-NL63 S1-CTD is a  $\beta$ -sandwich consisting of two three-stranded antiparallel  $\beta$ -sheets. It differs from the core structure of SARS-CoV S1-CTD, which consists of a single-layer, five-stranded  $\beta$ -sheet. The RBMs of HCoV-NL63 S1-CTD are three short, discontinuous loops. They differ from the RBM of SARS-CoV S1-CTD, which is a long, continuous subdomain. Nevertheless, HCoV-NL63 and SARS-CoV S1-CTDs share the same structural topology (connectivity of secondary structural elements) (42) (Figure 4c,d). Despite their different structures, HCoV-NL63 and SARS-CoV S1-CTDs bind to the same VBMs on human ACE2 (Figure 4e,f). Between the two SARS-CoV-binding hot spots on human ACE2, the hot spot centering on Lys353 also plays a critical role in HCoV-NL63 binding (59). Consequently, as with SARS-CoV, entry of HCoV-NL63 into mouse cells is inefficient due to the presence of His353 on mouse ACE2 (48, 83). These studies demonstrate that viral RBDs with different structures can bind to a common virus-binding hot spot on the same protein receptor.

The structure of alphacoronavirus PRCV S1-CTD complexed with porcine APN, when compared with HCoV-NL63, presented another example of how two similar coronavirus RBDs bind to different protein receptors (84) (Figure 4a,b). Like HCoV-NL63 S1-CTD, PRCV S1-CTD contains a  $\beta$ -sandwich core structure and three RBM loops. The core structures of PRCV and HCoV-NL63 S1-CTDs are similar to each other, but their RBMs are divergent, leading to different receptor specificities. The ectodomain of APN has a seahorse-shaped structure and forms a head-to-head dimer (85, 86). The VBMs are located on the outer surface of APN, away from the buried APN catalytic site. Several other alphacoronaviruses, such as TGEV, PEDV, human coronavirus 229E, feline coronavirus, and canine coronavirus, recognize APN from their natural host as their receptor (22–25, 87). These APN-recognizing alphacoronaviruses, except for PEDV, have been shown to also recognize feline APN, suggesting transmission of feline coronavirus from cats to other mammals (87). These studies showed again that similar viral RBDs with a conserved core structure can recognize different protein receptors through structurally divergent RBMs.

The above studies provide insight into the evolution of coronavirus S1-CTDs (19). Although the core structures of alpha- and betacoronavirus S1-CTDs are a  $\beta$ -sandwich and a single-layer  $\beta$ -sheet, respectively, they share the same structural topology, suggesting a common evolutionary origin. The S1-CTDs from different genera likely have undergone extensive divergent evolution to attain different core structures. The three RBM loops of alphacoronavirus S1-CTDs might have further diverged into ACE2-binding RBMs in HCoV-NL63 and APN-binding RBMs in PRCV. The RBM subdomain of betacoronavirus S1-CTDs might also have diverged into ACE2-binding RBM in SARS-CoV and DPP4-binding RBM in MERS-CoV. Despite their different structures, alphacoronavirus HCoV-NL63 and betacoronavirus SARS-CoV S1-CTDs bind to a common region on ACE2, possibly driven by the common virus-binding hot spot on ACE2. The tertiary structures of the S1-CTDs from gamma- and deltacoronaviruses are unavailable but are likely related to the folds of alpha- and betacoronavirus S1-CTDs. The complex evolutionary relationships among the S1-

CTDs from different genera reflect the heavy evolutionary pressure on this domain, which is discussed in more detail in this review.

## RECEPTOR RECOGNITION BY CORONAVIRUS S1-NTDS

The structure of betacoronavirus MHV S1-NTD complexed with murine CEACAM1 provided the first atomic view of coronavirus S1-NTDs (88) (Figure 5a). MHV S1-NTD consists of a  $\beta$ -sandwich core structure and a ceiling-like structure on top of it. The core structure contains two antiparallel  $\beta$ -sheets, one with six  $\beta$ -strands and the other with seven. MHV S1-NTD has the same structural fold as human galectins (galactose-binding lectins) (Figure 5a,c,e,f). The RBMs are located on the outer surface of the ceiling-like structure. On the other hand, CEACAM1 contains either two or four immunoglobulin (Ig) domains (89,90). The VBMs are located on the membranedistal surface of the N-terminal Ig domain of CEACAM1. Despite its galectin fold, MHV S1-NTD binds to CEACAM1 through exclusive protein-protein interactions. Structural and mutagenesis studies have identified two critical hydrophobic patches at the S1-NTD/CEACAM1 interface (88, 90–93). Critical RBM residues are conserved in the S1-NTDs from different MHV strains, including hepatotropic strain A59 and neurotropic strain JHM, allowing these MHV strains to use CEACAM1 as their receptor (94). Several critical VBM residues differ between two forms of CEACAM1 encoded by mice, CEACAM1a and CEACAM1b, rendering CEACAM1a, but not CEACAM1b, as an effective receptor for MHV (95–97). CEACAM1a molecules from mouse, cattle, and human also differ in several critical VBM residues, presenting a barrier for cross-species transmissions of MHV (88). These studies reveal a surprising galectin fold of MHV S1-NTD and provide insight into the host range and tissue tropism of MHV.

The structure of betacoronavirus BCoV S1-NTD illustrated a functional coronavirus spike lectin domain (43) (Figure 5b). BCoV S1-NTD has a galectin fold similar to that of MHV S1-NTD. However, unlike MHV S1-NTD, which recognizes a protein receptor, BCoV S1-NTD recognizes a sugar receptor. Mutagenesis studies have identified the sugar-binding pocket in the cavity surrounded by both the core structure and the ceiling-like structure on top of it. The sugar-binding site in BCoV S1-NTD overlaps with that in human galectins, although galectins do not have the ceiling-like structure and consequently their sugar-binding site is open (98). BCoV S1-NTD does not recognize galactose as galectins do. Instead, it recognizes 5-*N*-acetyl-9-*O*-acetylneuraminic acid (Neu5,9Ac2) (30, 43). The same sugar receptor is also recognized by human coronavirus OC43 (43, 99). OC43 and BCoV are closely related genetically, and OC43 might have resulted from zoonotic spillover of BCoV (100, 101). Because Neu5,9Ac2 is widely expressed in mammalian tissues (102), recognition of this sugar receptor might have played a role in the cattle-to-human transmission of BCoV. In contrast, despite the structural similarity between MHV and BCoV S1-NTDs, MHV S1-NTD binds CEACAM1 but not sugar (43, 88). MHV S1-NTD does not bind sugar, because a critical sugar-binding loop in BCoV S1-NTD has a different conformation in MHV S1-NTD. Similarly, BCoV S1-NTD does not bind CEACAM1, because the CEACAM-binding RBMs in MHV S1-NTD have undergone conformational changes in BCoV S1-NTD. Therefore, despite their common galectin fold, betacoronavirus S1-NTDs can recognize either a protein receptor or a sugar receptor depending on the conformation of their RBMs.

The structures of S1-NTDs from alpha-, gamma-, and deltacoronaviruses are unavailable, but on the basis of the following observations, they probably all have a galectin fold. First, the related structural topology between alpha- and betacoronavirus S1-CTDs suggests that the S1 subunits across different genera have a common evolutionary origin (42). Second, the S1-NTDs from the alphacoronaviruses TGEV and PEDV and the gammacoronavirus IBV all recognize sugar receptors, although TGEV S1-NTD recognizes *N*-glycolylneuraminic acid (Neu5Gc) and *N*-acetylneuraminic acid (Neu5Ac), PEDV S1-NTD recognizes Neu5Ac, and IBV S1-NTD recognizes Neu5Gc (23, 31, 34, 44). Therefore, the S1-NTDs from different genera are likely all evolutionarily and structurally related.

Based on the above studies, the following evolutionary scenario has been proposed for coronavirus S1-NTDs (19). Through gene capture, ancestral coronaviruses might have acquired a host galectin, which would become the S1-NTD of their spikes. Consequently, coronaviruses would recognize sugar receptors for cell entry. To aid viral release from infected cells, some coronaviruses would also evolve a hemagglutinin-esterase protein (HE) as a receptor-destroying enzyme. Later, coronavirus S1-NTDs would evolve a ceiling-like structure that could protect their sugar-binding site from host immune surveillance; this ceiling-like structure is absent in galectins because as host proteins, galectins are not recognized by the host immune system. The outer surface of the ceiling-like structure in MHV would further evolve structural features that could function as RBMs and recognize CEACAM1. Because protein receptors in general provide higher affinity and specificity for viral attachment than sugar receptors do, the sugar-binding function of MHV S1-NTD would become dispensable and be lost. The S1-NTDs of some other contemporary coronaviruses, such as the alphacoronaviruses TGEV and PEDV, the betacoronaviruses BCoV and OC43, and the gammacoronavirus IBV, have retained the lectin function, but their sugar specificities have diverged. The galectin-like domain has also been found in a number of other viral spikes (103) (Figure 5d,g), including influenza virus HA1, rotavirus VP4, and the adenovirus galectin domain. These viral galectin-like domains display diverse sugar-binding modes, but their sugar-binding sites are all located in cavities, possibly to evade host immune surveillance. Overall, it appears to be a successful strategy for viruses to acquire a host lectin and evolve it into viral RBDs with novel specificity for a protein receptor or altered specificity for a different sugar receptor.

## STRUCTURAL MECHANISM FOR MEMBRANE FUSION BY CORONAVIRUS SPIKE PROTEINS

The coronavirus spike is believed to be a member of the class I viral membrane fusion proteins that also include those from influenza virus, human immunodeficiency virus (HIV), and Ebola virus (Figure 6a). Among these proteins, the hemagglutinin glycoprotein (HA) of the influenza virus is arguably the best studied (104, 105). HA is expressed as a single-chain precursor. During molecular maturation, it trimerizes and is cleaved by host proteases into receptor-binding subunit HA1 and membrane-fusion subunit HA2, which still associate together through noncovalent interactions (106, 107). This prefusion state of HA on the newly packaged virions is a proteolytically primed and metastable trimer. During cell entry, HA1 binds to a sugar receptor on the host cell surface for viral attachment, and then HA1

dissociates and HA2 undergoes a dramatic conformational change to transition to the postfusion state. During this transition, three pairs of heptad repeat regions HR-N and HR-C in trimeric HA2 form a six-helix bundle structure. Three previously buried hydrophobic fusion peptides in trimeric HA2 become exposed and insert into the target host membrane. The fusion peptides and transmembrane anchors are eventually positioned on the same end of the six-helix bundle, bringing the viral and host membranes together to fuse. Because the six-helix bundle structure is energetically stable, a large amount of energy is released during the conformational transition of HA, driving membrane fusion forward. However, an initial energy barrier for the conformational transition of HA must be overcome through the aforementioned proteolytic priming and one or more subsequent triggers. These triggers can be receptor binding (e.g., HIV) (108), low pH (e.g., influenza virus) (109), or a combination of the two (e.g., avian leucosis virus) (110). Consequently, membrane fusion occurs either on the host cell surface (e.g., HIV) or in the endosomes (e.g., influenza virus).

The prefusion structures of betacoronavirus MHV and HKU1 spikes were recently determined using cryo-electron microscopy (15, 16) (Figure 2a). The overall architecture of the prefusion coronavirus spikes is similar to, albeit significantly larger and more complex than, that of influenza virus HA. In each spike, three S1 heads sit on top of a trimeric S2 stalk, preventing S2 from undergoing conformational transitions. Between the two major S1 domains, S1-CTD is located at the very top of the spike, whereas S1-NTD directly contacts and structurally constrains S2. In the S2 stalk, HR-N forms several helices and arranges itself along the central threefold symmetry axis of trimeric S2, whereas HR-C is poorly ordered. Unlike the fusion peptide in influenza virus HA, which is located at the N terminus of HA2, the fusion peptide in coronavirus spikes is located downstream from the N terminus of S2 and is hence an internal fusion peptide. The coronavirus fusion peptide forms a short helix and a loop, with most of the hydrophobic residues buried inside the prefusion structure. Two proteolysis sites are essential for the conformational transition of S2, one at the S1/S2 boundary and the other at the N terminus of the internal fusion peptide (111, 112). Like prefusion influenza virus HA, the prefusion coronavirus spike is in a metastable state and primed to undergo conformational transitions for membrane fusion.

Atomic models of full-length postfusion coronavirus spikes are not available, but a negative-stain electron microscopy study on SARS-CoV spike provided a direct view of its conformational transition that is likely associated with membrane fusion during virus entry (18) (Figure 6b). *In vitro* triggers (e.g., trypsin cleavage and urea incubation) induce the prefusion SARS-CoV spike to transition to its postfusion state, in which S1 dissociates and S2 forms a dumbbell-shaped structure with a rod-like structure in the middle and a globular structure at each end. These trimeric S2 molecules further associate at one end to form rosettes in solution. Comparison with influenza virus HA suggests that the rod-like structure in the middle likely represents the six-helix bundle formed by HR-N and HR-C, whereas the globular structures at the two ends likely correspond to the regions N-terminal to HR-N and between HR-N and HR-C, respectively (Figures 1c and 6c). Three hydrophobic fusion peptides, located N-terminal to HR-N, were previously buried in the prefusion spike but become exposed in the postfusion S2 and associate to form rosettes in solution (they would insert into host membranes, were the membranes present). Crystal structures of the six-helix bundle have been determined for a number of coronaviruses such as MHV, SARS-CoV,

MERS-CoV, and HCoV-NL63 (113–119) (Figures 1d and 6c). Compared with influenza virus HA, the six-helix bundle formed by coronavirus HR-N and HR-C is unusually long (18, 117), indicating the abundant amount of energy that can be released during the conformational transition of S2 and available for use in membrane fusion. Overall, these studies reveal that coronavirus spikes fuse membranes using the same structural mechanism as other class I membrane fusion proteins, but not for lack of some unique features such as their large size, internal fusion peptide, double cleavage sites, and long six-helix bundle.

## TRIGGERS FOR MEMBRANE FUSION BY CORONAVIRUS SPIKE PROTEINS

The triggers for coronavirus spikes to undergo conformational transitions demonstrate a more complex pattern than many other class I membrane fusion proteins, probably a reflection of their unique structural features discussed above. For example, although influenza virus HA is primed by proteolysis during virus packaging, many coronavirus spikes are not. Instead, coronavirus spikes are often subjected to proteolysis later in the cell entry process, sometimes after receptor binding. Thus, proteolysis of coronavirus spikes can lead directly to membrane fusion and thereby serves as an essential trigger for membrane fusion (111, 112). The host proteases that cleave coronavirus spikes mainly come from four different stages of the virus infection cycle: (a) proprotein convertases (e.g., furin) during virus packaging in virus-producing cells, (b) extracellular proteases (e.g., elastase) after virus release into extracellular space, (c) cell surface proteases [e.g., type II transmembrane serine protease (TMPRSS2)] after virus attachment to virus-targeting cells, and (d) lysosomal proteases (e.g., cathepsin L and cathepsin B) after virus endocytosis in virus-targeting cells (120) (Figure 7). In addition to proteolysis, traditional triggers such as receptor binding and low pH may also play a role in membrane fusion. Here, I discuss detailed triggers for membrane fusion by the spikes from three representative coronaviruses.

As the prototypic coronavirus, MHV has been extensively examined for its cell entry mechanism. The findings are complicated and in some cases contradictory. First, MHV spike is cleaved by proprotein convertases during virus packaging in the virus-producing cells (121). This proteolysis is critical for MHV entry into virus-targeting cells. Second, the binding of CEACAM1 triggers the conformational transition of MHV spike and hence membrane fusion. This is supported by the observations that incubation of MHV spike with recombinant soluble CEACAM1 led to enhanced hydrophobicity of MHV S2 and the appearance of a protease-resistant S2 fragment (122, 123). These observations indicated the exposure of fusion peptides and formation of the six-helix bundle, respectively, in postfusion S2. Third, there have been contradictory reports about whether MHV enters target cells at the cell membrane or through endocytosis and whether MHV spike undergoes conformational transitions at low, neutral, or even elevated pH (123–125). This may depend on the MHV strains examined or experimental approaches used in the studies. The roles of pH and endocytosis in MHV entry still need to be further clarified. Interestingly, the neurotropic strain MHV-JHM can mediate virus entry into host cells that do not express CEACAM1 (126–128). This receptor-independent entry by MHV-JHM is unique among viruses. Biochemical characterization of MHV-JHM spike suggested that it is more labile than the spikes from other MHV strains, meaning that it undergoes conformational transitions spontaneously in the absence of the receptor (94, 129, 130). It is believed that

MHV-JHM is able to infect neural cells where CEACAM1 expression level is very low, at least in part because its spike can mediate receptor-independent entry (131, 132). Taken together, the membrane fusion mechanism of MHV spike depends on both proteolysis and receptor binding, and it may or may not depend on the low pH of endosomes; in addition, receptor-independent membrane fusion by MHV-JHM spike contributes to the neutral tropism of MHV-JHM.

Research on the cell entry mechanism of SARS-CoV has led to novel findings. First, SARS-CoV spike is not cleaved by proprotein convertases during virus packaging and hence remains intact on mature virions (133, 134). Instead, SARS-CoV enters host cells through endocytosis, and its spike is processed by lysosomal proteases (e.g., cathepsin L and cathepsin B) (135–137). This is supported by the observation that inhibitors against either endosomal acidification or lysosomal cysteine proteases block SARS-CoV entry. However, low pH itself is not a trigger for SARS-CoV entry. This is supported by the observation that when expressed on the cell surface and cleaved by exogenous proteases, SARS-CoV spike can mediate cell-cell fusion with ACE2-expressing cells at neutral pH (136). Thus, the role of low pH in SARS-CoV entry is to activate lysosomal proteases, which further activate SARS-CoV spike for membrane fusion. This is different from influenza virus HA, which is activated through binding protons in the low-pH environment of endosomes. Second, in addition to lysosomal proteases, both extracellular proteases (e.g., elastases in the respiratory tract) and cell surface proteases (e.g., TMPRSS2 on the surface of lung cells) also activate SARS-CoV spike for membrane fusion (138–142). Due to their cell and tissue specificities, these proteases likely contribute to the respiratory tract and lung tropism of SARS-CoV. Third, in addition to the cleavage site at the S1/S2 boundary, a second site, S2', has been identified at the N terminus of the internal fusion peptide within S2 (143, 144). Whereas the cleavage at the S1/S2 boundary removes the structural constraint of S1 on S2, the cleavage at the S2' site releases the internal fusion peptide for insertion into target membranes (Figures 1c and 2b). Fourth, it is not clear whether the binding of receptor ACE2 is a trigger for SARS-CoV spike to fuse membranes. Two electron microscopy studies observed no or moderate conformational changes of SARS-CoV spike associated with ACE2 binding (18, 145). However, other studies suggested that ACE2 binding triggers a conformational change in SARS-CoV spike, which exposes previously cryptic protease sites for cleavage (135, 146). The role of ACE2 binding in triggering membrane fusion waits to be further investigated. Nevertheless, SARS-CoV entry does not depend on low pH, but it requires at least two protease cleavages in the spike by lysosomal proteases, extracellular proteases, or cell surface proteases.

The overall cell entry mechanism of MERS-CoV is similar to that of SARS-CoV. Like SARS-CoV spike, MERS-CoV spike must be cleaved at both the S1/S2 boundary and the S2' site for membrane fusion to occur (147). MERS-CoV also enters host cells through endocytosis and is activated by lysosomal cysteine proteases for membrane fusion (27, 148). Moreover, extracellular proteases and cell surface proteases help activate MERS-CoV entry (148–150). Unlike SARS-CoV, MERS-CoV spike is cleaved by host proprotein convertases during virus packaging (27, 151). Interestingly, despite recognizing the same receptor DPP4, MERS-CoV and HKU4 spikes differ in their activities to mediate virus entry: HKU4 spike mediates virus entry into bat cells but not human cells, whereas MERS-CoV spike mediates

virus entry into both bat and human cells (152). Two residue differences have been identified between MERS-CoV and HKU4 spikes that account for this functional difference (152); they allow MERS-CoV spike, but not HKU4 spike, to be activated by human proprotein convertases and lysosomal cysteine proteases. Thus, the corresponding two mutations played a critical role in the transmission of MERS-CoV from its likely natural reservoir, bats, to humans, either directly or through intermediate host camels. On the other hand, HKU4 spike can be activated by bat lysosomal proteases but not human lysosomal proteases, suggesting that human and bat lysosomal proteases process viral spikes differently. These studies on MERS-CoV entry reveal that different activities of spike-processing proteases from different hosts can pose a barrier for cross-species transmissions of viruses.

In sum, proteolysis has been established as an essential trigger for coronavirus spikes to fuse membranes, as cleavages at the S1/S2 boundary and S2' site can remove the structural constraint of S1 on S2 and release the internal fusion peptide, respectively. Among the host proteases, lysosomal proteases provide the most reliable source for spike processing because they are ubiquitous and abundant in many cell types. The availability of some other proteases (e.g., proprotein convertases, extracellular proteases, and cell surface proteases) depends on the types of cells and tissues, regulating tissue tropisms of coronaviruses. Moreover, protease activities from different host species may vary, regulating host ranges of coronaviruses. Some other triggers for coronavirus entry (e.g., receptor binding and low pH) may depend on specific coronaviruses or different strains of the same coronavirus. The overall goal of these triggers is to overcome the energy barrier for the conformational transition of coronavirus spikes.

## EVOLUTION OF CORONAVIRUS SPIKE PROTEINS

Coronavirus spikes, like other class I viral membrane fusion proteins, are amazing molecules. They single-handedly lead coronaviruses to enter host cells by first binding to a receptor on the host cell surface and then fusing the viral and host membranes. They exist in two distinct conformations: The prefusion trimeric spike contains three receptor-binding S1 heads and a trimeric membranefusion S2 stalk, whereas the postfusion trimeric S2 is a six-helix bundle with exposed fusion peptides. The transition of the spikes from prefusion to postfusion conformation is regulated by a variety of triggers. Both receptor recognition and membrane fusion are critical determinants of the host range and tissue tropism of coronaviruses. How have these complex structures and functions of coronavirus spikes evolved?

Structure determinations of coronavirus S1 domains provide insight into the evolution of coronavirus S1. The finding that betacoronavirus S1-NTDs have a galectin fold indicates a host origin of coronavirus S1-NTDs. The origin of coronavirus S1-CTDs is less clear. Alphacoronavirus S1-CTDs and host galectins also share some similarity in the structural topologies of their ( $\beta$ -sandwich folds (Figure 8a), although this similarity is less significant than that between S1-NTDs and host galectins (Figure 5e,f).  $\beta$ -Sandwich folds are common and stable structures, and two  $\beta$ -sandwich folds may result from convergent evolution with protein stability as the evolutionary driving force. However, two  $\beta$ -sandwich folds with related structural topologies may indicate a common evolutionary ancestor when a

significant number of their constituent  $\beta$ -strands are connected in the same order. Thus, there is a possibility that S1-CTD and host galectins are evolutionarily related. One possible scenario is that after S1-NTD was generated through gene capture, S1-CTD was generated through gene duplication of S1-NTD (Figure 8b). S1-CTDs appear to evolve at a quickened pace, as evidenced by the different tertiary structures between alpha- and betacoronavirus S1-CTDs. This may be associated with their location on the very top of the prefusion trimeric spike (Figure 2), which is the most protruding and exposed area on virions. Hence, S1-CTDs are under heavy selective pressure to escape host immune surveillance. The resulting fast-paced evolution of S1-CTDs may have permanently erased their evolutionary traces, except for the limited information from their structural topology. Whether S1-CTDs originated from host galectins or not, the two-domain structure of S1 gives coronaviruses two potential receptor-binding domains: The more structurally and functionally conserved S1-NTD uses sugar as the fallback receptor, whereas the more aggressively evolving S1-CTD exploits novel protein receptors (Figure 8).

The structural and functional similarities between coronavirus S2 and other class I viral membrane fusion proteins are profound. These proteins all exist in prefusion and postfusion conformations. Their prefusion structures can be triggered in a number of similar ways, undergo similar conformational rearrangement, and transition to highly similar postfusion six-helix bundle structures with exposed fusion peptides. Although it cannot be completely ruled out that the same membrane fusion mechanism evolved independently in these viruses, the complexity and intricacy of this mechanism indicate that class I viral membrane fusion proteins likely share a common evolutionary ancestor.

Which function evolved first for coronaviruses: receptor recognition by S1, membrane fusion by S2, or both simultaneously? Because coronaviruses must enter cells for replication, membrane fusion is the central function of coronavirus spikes. Receptor recognition, though, can specifically attach coronaviruses to host cell surfaces and position the spikes within striking distance of target host membranes. The spike of neurotropic strain MHV-JHM can mediate receptor-independent virus entry into cells that do not express its receptor, suggesting that receptor binding can be circumvented under some extreme situations. Therefore, the primordial form of coronavirus spikes might contain S2 only (Figure 8b). Such a primordial spike might function inefficiently because the ancestral virus would have to diffuse nonspecifically to the close proximity of target cells so that membrane fusion could occur. Later, the spike would evolve a galectin-like S1-NTD through gene capture, which would enhance its efficiency in mediating virus entry. Next, the spike would evolve an S1-CTD through gene duplication of its S1-NTD or some other mechanism, further strengthening its receptor recognition function. Understanding the structure and function of coronavirus spikes and their evolution can enhance our understanding of the origin of viruses and the evolutionary relationship between viruses and host cells.

## Acknowledgments

This work was supported by the National Institutes of Health (R01AI089728, R01AI110700).

## LITERATURE CITED

1. Ksiazek TG, Erdman D, Goldsmith CS, Zaki SR, Peret T, et al. A novel coronavirus associated with severe acute respiratory syndrome. *N Engl J Med*. 2003; 348:1953–66. [PubMed: 12690092]
2. Peiris JSM, Lai ST, Poon LLM, Guan Y, Yam LYC, et al. Coronavirus as a possible cause of severe acute respiratory syndrome. *Lancet*. 2003; 361:1319–25. [PubMed: 12711465]
3. Marra MA, Jones SJM, Astell CR, Holt RA, Brooks-Wilson A, et al. The genome sequence of the SARS-associated coronavirus. *Science*. 2003; 300:1399–404. [PubMed: 12730501]
4. Rota PA, Oberste MS, Monroe SS, Nix WA, Campagnoli R, et al. Characterization of a novel coronavirus associated with severe acute respiratory syndrome. *Science*. 2003; 300:1394–99. [PubMed: 12730500]
5. Zaki AM, van Boheemen S, Bestebroer TM, Osterhaus A, Fouchier RAM. Isolation of a novel coronavirus from a man with pneumonia in Saudi Arabia. *N Engl J Med*. 2012; 367:1814–20. [PubMed: 23075143]
6. de Groot RJ, Baker SC, Baric RS, Brown CS, Drosten C, et al. Middle East respiratory syndrome coronavirus (MERS-CoV): announcement of the Coronavirus Study Group. *J Virol*. 2013; 87:7790–92. [PubMed: 23678167]
7. Mole B. Deadly pig virus slips through US borders. *Nature*. 2013; 499:388. [PubMed: 23887408]
8. Stevenson GW, Hoang H, Schwartz KJ, Burrough ER, Sun D, et al. Emergence of porcine epidemic diarrhea virus in the United States: clinical signs, lesions, and viral genomic sequences. *J Vet Diagn Investig*. 2013; 25:649–54. [PubMed: 23963154]
9. Chen Q, Li G, Stasko J, Thomas JT, Stensland WR, et al. Isolation and characterization of porcine epidemic diarrhea viruses associated with the 2013 disease outbreak among swine in the United States. *J Clin Microbiol*. 2014; 52:234–43. [PubMed: 24197882]
10. Enjuanes L, Almazan F, Sola I, Zuniga S. Biochemical aspects of coronavirus replication and virus-host interaction. *Annu Rev Microbiol*. 2006; 60:211–30. [PubMed: 16712436]
11. Perlman S, Netland J. Coronaviruses post-SARS: update on replication and pathogenesis. *Nat Rev Microbiol*. 2009; 7:439–50. [PubMed: 19430490]
12. Graham RL, Baric RS. Recombination, reservoirs, and the modular spike: mechanisms of coronavirus cross-species transmission. *J Virol*. 2010; 84:3134–46. [PubMed: 19906932]
13. Li F. Receptor recognition and cross-species infections of SARS coronavirus. *Antivir Res*. 2013; 100:246–54. [PubMed: 23994189]
14. Li WH, Wong SK, Li F, Kuhn JH, Huang IC, et al. Animal origins of the severe acute respiratory syndrome coronavirus: insight from ACE2-S-protein interactions. *J Virol*. 2006; 80:4211–19. [PubMed: 16611880]
15. Kirchdoerfer RN, Cottrell CA, Wang N, Pallesen J, Yassine HM, et al. Pre-fusion structure of a human coronavirus spike protein. *Nature*. 2016; 531:118–21. [PubMed: 26935699]
16. Walls AC, Tortorici MA, Bosch BJ, Frenz B, Rottier PJ, et al. Cryo-electron microscopy structure of a coronavirus spike glycoprotein trimer. *Nature*. 2016; 531:114–17. [PubMed: 26855426]
17. Beniac DR, Andonov A, Grudeski E, Booth TF. Architecture of the SARS coronavirus prefusion spike. *Nat Struct Mol Biol*. 2006; 13:751–52. [PubMed: 16845391]
18. Li F, Berardi M, Li WH, Farzan M, Dormitzer PR, Harrison SC. Conformational states of the severe acute respiratory syndrome coronavirus spike protein ectodomain. *J Virol*. 2006; 80:6794–800. [PubMed: 16809285]
19. Li F. Receptor recognition mechanisms of coronaviruses: a decade of structural studies. *J Virol*. 2015; 89:1954–64. [PubMed: 25428871]
20. Li WH, Moore MJ, Vasilieva N, Sui JH, Wong SK, et al. Angiotensin-converting enzyme 2 is a functional receptor for the SARS coronavirus. *Nature*. 2003; 426:450–54. [PubMed: 14647384]
21. Hofmann H, Pyrc K, van der Hoek L, Geier M, Berkhout B, Pohlmann S. Human coronavirus NL63 employs the severe acute respiratory syndrome coronavirus receptor for cellular entry. *PNAS*. 2005; 102:7988–93. [PubMed: 15897467]
22. Delmas B, Gelfi J, Lharidon R, Vogel LK, Sjostrom H, et al. Aminopeptidase-N is a major receptor for the enteropathogenic coronavirus TGEV. *Nature*. 1992; 357:417–20. [PubMed: 1350661]

23. Liu C, Tang J, Ma Y, Liang X, Yang Y, et al. Receptor usage and cell entry of porcine epidemic diarrhea coronavirus. *J Virol*. 2015; 89:6121–25. [PubMed: 25787280]
24. Li BX, Ge JW, Li YJ. Porcine aminopeptidase N is a functional receptor for the PEDV coronavirus. *Virology*. 2007; 365:166–72. [PubMed: 17467767]
25. Delmas B, Gelfi J, Sjostrom H, Noren O, Laude H. Further characterization of aminopeptidase-N as a receptor for coronaviruses. *Adv Exp Med Biol*. 1993; 342:293–98. [PubMed: 7911642]
26. Raj VS, Mou HH, Smits SL, Dekkers DHW, Muller MA, et al. Dipeptidyl peptidase 4 is a functional receptor for the emerging human coronavirus-EMC. *Nature*. 2013; 495:251–54. [PubMed: 23486063]
27. Yang Y, Du L, Liu C, Wang L, Ma C, et al. Receptor usage and cell entry of bat coronavirus HKU4 provide insight into bat-to-human transmission of MERS coronavirus. *PNAS*. 2014; 111:12516–21. [PubMed: 25114257]
28. Dveksler GS, Pensiero MN, Cardellicchio CB, Williams RK, Jiang GS, et al. Cloning of the mouse hepatitis-virus (MHV) receptor: expression in human and hamster cell lines confers susceptibility to MHV. *J Virol*. 1991; 65:6881–91. [PubMed: 1719235]
29. Williams RK, Jiang GS, Holmes KV. Receptor for mouse hepatitis virus is a member of the carcinoembryonic antigen family of glycoproteins. *PNAS*. 1991; 88:5533–36. [PubMed: 1648219]
30. Schultze B, Gross HJ, Brossmer R, Herrler G. The S protein of bovine coronavirus is a hemagglutinin recognizing 9-*O*-acetylated sialic acid as a receptor determinant. *J Virol*. 1991; 65:6232–37. [PubMed: 1920630]
31. Schultze B, Cavanagh D, Herrler G. Neuraminidase treatment of avian infectious bronchitis coronavirus reveals a hemagglutinating activity that is dependent on sialic acid-containing receptors on erythrocytes. *Virology*. 1992; 189:792–94. [PubMed: 1322604]
32. Cavanagh D, Davis PJ. Coronavirus IBV: removal of spike glycopolypeptide S1 by urea abolishes infectivity and hemagglutination but not attachment to cells. *J Gen Virol*. 1986; 67:1443–48. [PubMed: 3014054]
33. Schwegmann-Wessels C, Herrler G. Sialic acids as receptor determinants for coronaviruses. *Glycoconj J*. 2006; 23:51–58. [PubMed: 16575522]
34. Krempf C, Schultze B, Laude H, Herrler G. Point mutations in the S protein connect the sialic acid binding activity with the enteropathogenicity of transmissible gastroenteritis coronavirus. *J Virol*. 1997; 71:3285–87. [PubMed: 9060696]
35. Liu C, Yang Y, Chen L, Lin YL, Li F. A unified mechanism for aminopeptidase N-based tumor cell motility and tumor-homing therapy. *J Biol Chem*. 2014; 289:34520–29. [PubMed: 25359769]
36. Mina-Osorio P. The moonlighting enzyme CD13: old and new functions to target. *Trends Mol Med*. 2008; 14:361–71. [PubMed: 18603472]
37. Boehm M, Nabel EG. Angiotensin-converting enzyme 2—a new cardiac regulator. *N Engl J Med*. 2002; 347:1795–97. [PubMed: 12456857]
38. Kameoka J, Tanaka T, Nojima Y, Schlossman SF, Morimoto C. Direct association of adenosine deaminase with a T cell activation antigen, CD26. *Science*. 1993; 261:466–69. [PubMed: 8101391]
39. Wesley UV, McGroarty M, Homoyouni A. Dipeptidyl peptidase inhibits malignant phenotype of prostate cancer cells by blocking basic fibroblast growth factor signaling pathway. *Cancer Res*. 2005; 65:1325–34. [PubMed: 15735018]
40. Hammarstrom S. The carcinoembryonic antigen (CEA) family: structures, suggested functions and expression in normal and malignant tissues. *Semin Cancer Biol*. 1999; 9:67–81. [PubMed: 10202129]
41. Dove A. The bittersweet promise of glycobiology. *Nat Biotechnol*. 2001; 19:913–17. [PubMed: 11581651]
42. Li F. Evidence for a common evolutionary origin of coronavirus spike protein receptor-binding subunits. *J Virol*. 2012; 86:2856–58. [PubMed: 22205743]
43. Peng GQ, Xu LQ, Lin YL, Chen L, Pasquarella JR, et al. Crystal structure of bovine coronavirus spike protein lectin domain. *J Biol Chem*. 2012; 287:41931–38. [PubMed: 23091051]

44. Promkuntod N, van Eijndhoven RE, de Vriese G, Grone A, Verheije MH. Mapping of the receptor-binding domain and amino acids critical for attachment in the spike protein of avian coronavirus infectious bronchitis virus. *Virology*. 2014; 448:26–32. [PubMed: 24314633]
45. Kubo H, Yamada YK, Taguchi F. Localization of neutralizing epitopes and the receptor-binding site within the amino-terminal 330 amino-acids of the murine coronavirus spike protein. *J Virol*. 1994; 68:5403–10. [PubMed: 7520090]
46. Wong SK, Li WH, Moore MJ, Choe H, Farzan M. A 193-amino acid fragment of the SARS coronavirus S protein efficiently binds angiotensin-converting enzyme 2. *J Biol Chem*. 2004; 279:3197–201. [PubMed: 14670965]
47. Lin HX, Fen Y, Wong G, Wang LP, Li B, et al. Identification of residues in the receptor-binding domain (RBD) of the spike protein of human coronavirus NL63 that are critical for the RBD-ACE2 receptor interaction. *J Gen Virol*. 2008; 89:1015–24. [PubMed: 18343844]
48. Hofmann H, Simmons G, Rennekamp AJ, Chaipan C, Gramberg T, et al. Highly conserved regions within the spike proteins of human coronaviruses 229E and NL63 determine recognition of their respective cellular receptors. *J Virol*. 2006; 80:8639–52. [PubMed: 16912312]
49. Godet M, Grosclaude J, Delmas B, Laude H. Major receptor-binding and neutralization determinants are located within the same domain of the transmissible gastroenteritis virus (coronavirus) spike protein. *J Virol*. 1994; 68:8008–16. [PubMed: 7525985]
50. Du L, Zhao G, Kou Z, Ma C, Sun S, et al. Identification of a receptor-binding domain in the S protein of the novel human coronavirus Middle East respiratory syndrome coronavirus as an essential target for vaccine development. *J Virol*. 2013; 87:9939–42. [PubMed: 23824801]
51. Mou H, Raj VS, van Kuppeveld FJ, Rottier PJ, Haagmans BL, Bosch BJ. The receptor binding domain of the new MERS coronavirus maps to a 231-residue region in the spike protein that efficiently elicits neutralizing antibodies. *J Virol*. 2013; doi: 10.1128/JVI.01277-13
52. Li F, Li WH, Farzan M, Harrison SC. Structure of SARS coronavirus spike receptor-binding domain complexed with receptor. *Science*. 2005; 309:1864–68. [PubMed: 16166518]
53. Li, F., Li, WH., Farzan, M., Harrison, SC. Interactions between SARS coronavirus and its receptor. In: Perlman, S., Holmes, KV., editors. *Nidoviruses: Toward Control of SARS and Other Nidovirus Diseases*. New York: Springer; 2006. p. 229-34.
54. Towler P, Staker B, Prasad SG, Menon S, Tang J, et al. ACE2 X-ray structures reveal a large hinge-bending motion important for inhibitor binding and catalysis. *J Biol Chem*. 2004; 279:17996–8007. [PubMed: 14754895]
55. Li WH, Zhang CS, Sui JH, Kuhn JH, Moore MJ, et al. Receptor and viral determinants of SARS-coronavirus adaptation to human ACE2. *EMBO J*. 2005; 24:1634–43. [PubMed: 15791205]
56. Guan Y, Zheng BJ, He YQ, Liu XL, Zhuang ZX, et al. Isolation and characterization of viruses related to the SARS coronavirus from animals in southern China. *Science*. 2003; 302:276–78. [PubMed: 12958366]
57. Li F. Structural analysis of major species barriers between humans and palm civets for severe acute respiratory syndrome coronavirus infections. *J Virol*. 2008; 82:6984–91. [PubMed: 18448527]
58. Wu KL, Peng GQ, Wilken M, Geraghty RJ, Li F. Mechanisms of host receptor adaptation by severe acute respiratory syndrome coronavirus. *J Biol Chem*. 2012; 287:8904–11. [PubMed: 22291007]
59. Wu K, Chen L, Peng G, Zhou W, Pennell CA, et al. A virus-binding hot spot on human angiotensin-converting enzyme 2 is critical for binding of two different coronaviruses. *J Virol*. 2011; 85:5331–37. [PubMed: 21411533]
60. Song HD, Tu CC, Zhang GW, Wang SY, Zheng K, et al. Cross-host evolution of severe acute respiratory syndrome coronavirus in palm civet and human. *PNAS*. 2005; 102:2430–35. [PubMed: 15695582]
61. Qu XX, Hao P, Song XJ, Jiang SM, Liu YX, et al. Identification of two critical amino acid residues of the severe acute respiratory syndrome coronavirus spike protein for its variation in zoonotic tropism transition via a double substitution strategy. *J Biol Chem*. 2005; 280:29588–95. [PubMed: 15980414]

62. Li WH, Greenough TC, Moore MJ, Vasilieva N, Somasundaran M, et al. Efficient replication of severe acute respiratory syndrome coronavirus in mouse cells is limited by murine angiotensin-converting enzyme 2. *J Virol.* 2004; 78:11429–33. [PubMed: 15452268]
63. Frieman M, Yount B, Agnihothram S, Page C, Donaldson E, et al. Molecular determinants of severe acute respiratory syndrome coronavirus pathogenesis and virulence in young and aged mouse models of human disease. *J Virol.* 2012; 86:884–97. [PubMed: 22072787]
64. Ge XY, Li JL, Yang XL, Chmura AA, Zhu G, et al. Isolation and characterization of a bat SARS-like coronavirus that uses the ACE2 receptor. *Nature.* 2013; 503:535–38. [PubMed: 24172901]
65. Menachery VD, Yount BL Jr, Debbink K, Agnihothram S, Gralinski LE, et al. A SARS-like cluster of circulating bat coronaviruses shows potential for human emergence. *Nat Med.* 2015; 21:1508–13. [PubMed: 26552008]
66. Li WD, Shi ZL, Yu M, Ren WZ, Smith C, et al. Bats are natural reservoirs of SARS-like coronaviruses. *Science.* 2005; 310:676–79. [PubMed: 16195424]
67. Lau SKP, Woo PCY, Li KSM, Huang Y, Tsoi HW, et al. Severe acute respiratory syndrome coronavirus-like virus in Chinese horseshoe bats. *PNAS.* 2005; 102:14040–45. [PubMed: 16169905]
68. Hou YX, Peng C, Yu M, Li Y, Han ZG, et al. Angiotensin-converting enzyme 2 (ACE2) proteins of different bat species confer variable susceptibility to SARS-CoV entry. *Arch Virol.* 2010; 155:1563–69. [PubMed: 20567988]
69. Lu G, Hu Y, Wang Q, Qi J, Gao F, et al. Molecular basis of binding between novel human coronavirus MERS-CoV and its receptor CD26. *Nature.* 2013; 500:227–31. [PubMed: 23831647]
70. Wang N, Shi X, Jiang L, Zhang S, Wang D, et al. Structure of MERS-CoV spike receptor-binding domain complexed with human receptor DPP4. *Cell Res.* 2013; 23:986–93. [PubMed: 23835475]
71. Chen Y, Rajashankar KR, Yang Y, Agnihothram SS, Liu C, et al. Crystal structure of the receptor-binding domain from newly emerged Middle East respiratory syndrome coronavirus. *J Virol.* 2013; 87:10777–83. [PubMed: 23903833]
72. Rasmussen HB, Branner S, Wiberg FC, Wagtmann N. Crystal structure of human dipeptidyl peptidase IV/CD26 in complex with a substrate analog. *Nat Struct Biol.* 2003; 10:19–25. [PubMed: 12483204]
73. Peck KM, Cockrell AS, Yount BL, Scobey T, Baric RS, Heise MT. Glycosylation of mouse DPP4 plays a role in inhibiting Middle East respiratory syndrome coronavirus infection. *J Virol.* 2015; 89:4696–99. [PubMed: 25653445]
74. Cockrell AS, Peck KM, Yount BL, Agnihothram SS, Scobey T, et al. Mouse dipeptidyl peptidase 4 is not a functional receptor for Middle East respiratory syndrome coronavirus infection. *J Virol.* 2014; 88:5195–99. [PubMed: 24574399]
75. Fukuma A, Tani H, Taniguchi S, Shimojima M, Saijo M, Fukushi S. Inability of rat DPP4 to allow MERS-CoV infection revealed by using a VSV pseudotype bearing truncated MERS-CoV spike protein. *Arch Virol.* 2015; 160:2293–300. [PubMed: 26138557]
76. Barlan A, Zhao J, Sarkar MK, Li K, McCray PB Jr, et al. Receptor variation and susceptibility to Middle East respiratory syndrome coronavirus infection. *J Virol.* 2014; 88:4953–61. [PubMed: 24554656]
77. Haagmans BL, Al Dhahiry SH, Reusken CB, Raj VS, Galiano M, et al. Middle East respiratory syndrome coronavirus in dromedary camels: an outbreak investigation. *Lancet Infect Dis.* 2014; 14:140–45. [PubMed: 24355866]
78. Alagaili AN, Briese T, Mishra N, Kapoor V, Sameroff SC, et al. Middle East respiratory syndrome coronavirus infection in dromedary camels in Saudi Arabia. *mBio.* 2014; 5:e00884–14. [PubMed: 24570370]
79. Annan A, Baldwin HJ, Corman VM, Klose SM, Owusu M, et al. Human  $\beta$ -coronavirus 2c EMC/2012-related viruses in bats, Ghana and Europe. *Emerg Infect Dis.* 2013; 19:456–59. [PubMed: 23622767]
80. Holmes KV, Dominguez SR. The new age of virus discovery: genomic analysis of a novel human  $\beta$ -coronavirus isolated from a fatal case of pneumonia. *mBio.* 2013; 4:e00548–12. [PubMed: 23300251]

81. Lau SK, Li KS, Tsang AK, Lam CS, Ahmed S, et al. Genetic characterization of *Betacoronavirus* lineage C viruses in bats reveals marked sequence divergence in the spike protein of *Pipistrellus* bat coronavirus HKU5 in Japanese pipistrelle: implications for the origin of the novel Middle East respiratory syndrome coronavirus. *J Virol.* 2013; 87:8638–50. [PubMed: 23720729]
82. Wang Q, Qi J, Yuan Y, Xuan Y, Han P, et al. Bat origins of MERS-CoV supported by bat coronavirus HKU4 usage of human receptor CD26. *Cell Host Microbe.* 2014; 16:328–37. [PubMed: 25211075]
83. Wu K, Li W, Peng G, Li F. Crystal structure of NL63 respiratory coronavirus receptor-binding domain complexed with its human receptor. *PNAS.* 2009; 106:19970–74. [PubMed: 19901337]
84. Reguera J, Santiago C, Mudgal G, Ordone D, Enjuanes L, Casanovas JM. Structural bases of coronavirus attachment to host aminopeptidase N and its inhibition by neutralizing antibodies. *PLOS Pathog.* 2012; 8:e1002859. [PubMed: 22876187]
85. Chen L, Lin YL, Peng G, Li F. Structural basis for multifunctional roles of mammalian aminopeptidase N. *PNAS.* 2012; 109:17966–71. [PubMed: 23071329]
86. Wong AH, Zhou D, Rini JM. The X-ray crystal structure of human aminopeptidase N reveals a novel dimer and the basis for peptide processing. *J Biol Chem.* 2012; 287:36804–13. [PubMed: 22932899]
87. Tusell SM, Schittone SA, Holmes KV. Mutational analysis of aminopeptidase N, a receptor for several group 1 coronaviruses, identifies key determinants of viral host range. *J Virol.* 2007; 81:1261–73. [PubMed: 17093189]
88. Peng GQ, Sun DW, Rajashankar KR, Qian ZH, Holmes KV, Li F. Crystal structure of mouse coronavirus receptor-binding domain complexed with its murine receptor. *PNAS.* 2011; 108:10696–701. [PubMed: 21670291]
89. Beauchemin N, Draber P, Dveksler G, Gold P, Gray-Owen S, et al. Redefined nomenclature for members of the carcinoembryonic antigen family. *Exp Cell Res.* 1999; 252:243–49. [PubMed: 11501563]
90. Tan KM, Zelus BD, Meijers R, Liu JH, Bergelson JM, et al. Crystal structure of murine sCEACAM1a[1,4]: a coronavirus receptor in the CEA family. *EMBOJ.* 2002; 21:2076–86.
91. Wessner DR, Shick PC, Lu JH, Cardellicchio CB, Gagneten SE, et al. Mutational analysis of the virus and monoclonal antibody binding sites in MHVR, the cellular receptor of the murine coronavirus mouse hepatitis virus strain A59. *J Virol.* 1998; 72:1941–48. [PubMed: 9499047]
92. Thackray LB, Turner BC, Holmes KV. Substitutions of conserved amino acids in the receptorbinding domain of the spike glycoprotein affect utilization of murine CEACAM1a by the murine coronavirus MHV-A59. *Virology.* 2005; 334:98–110. [PubMed: 15749126]
93. Leparc-Goffart I, Hingley ST, Chua MM, Jiang XH, Lavi E, Weiss SR. Altered pathogenesis of a mutant of the murine coronavirus MHV-A59 is associated with a Q159L amino acid substitution in the spike protein. *Virology.* 1997; 239:1–10. [PubMed: 9426441]
94. Tsai JC, Zelus BD, Holmes KV, Weiss SR. The N-terminal domain of the murine coronavirus spike glycoprotein determines the CEACAM1 receptor specificity of the virus strain. *J Virol.* 2003; 77:841–50. [PubMed: 12502800]
95. Ohtsuka N, Taguchi F. Mouse susceptibility to mouse hepatitis virus infection is linked to viral receptor genotype. *J Virol.* 1997; 71:8860–63. [PubMed: 9343248]
96. Ohtsuka N, Yamada YK, Taguchi F. Difference in virus-binding activity of two distinct receptor proteins for mouse hepatitis virus. *J Gen Virol.* 1996; 77:1683–92. [PubMed: 8760415]
97. Hirai A, Ohtsuka N, Ikeda T, Taniguchi R, Blau D, et al. Role of mouse hepatitis virus (MHV) receptor murine CEACAM1 in the resistance of mice to MHV infection: studies of mice with chimeric mCEACAM1a and mCEACAM1b. *J Virol.* 2010; 84:6654–66. [PubMed: 20410265]
98. Seetharaman J, Kanigsberg A, Slaaby R, Leffler H, Barondes SH, Rini JM. X-ray crystal structure of the human galectin-3 carbohydrate recognition domain at 2.1-Å resolution. *J Biol Chem.* 1998; 273:13047–52. [PubMed: 9582341]
99. Kunkel F, Herrler G. Structural and functional-analysis of the surface protein of human coronavirus OC43. *Virology.* 1993; 195:195–202. [PubMed: 8317096]

100. Vijgen L, Keyaerts E, Lemey P, Maes P, van Reeth K, et al. Evolutionary history of the closely related group 2 coronaviruses: porcine hemagglutinating encephalomyelitis virus, bovine coronavirus, and human coronavirus OC43. *J Virol.* 2006; 80:7270–74. [PubMed: 16809333]
101. Vijgen L, Keyaerts E, Moes E, Thoelen I, Wollants E, et al. Complete genomic sequence of human coronavirus OC43: molecular clock analysis suggests a relatively recent zoonotic coronavirus transmission event. *J Virol.* 2005; 79:1595–604. [PubMed: 15650185]
102. Klein A, Krishna M, Varki NM, Varki A. 9-*O*-acetylated sialic acids have widespread but selective expression: analysis using a chimeric dual-function probe derived from influenza C hemagglutinin-esterase. *PNAS.* 1994; 91:7782–86. [PubMed: 8052660]
103. Chen L, Li F. Structural analysis of the evolutionary origins of influenza virus hemagglutinin and other viral lectins. *J Virol.* 2013; 87:4118–20. [PubMed: 23365425]
104. Eckert DM, Kim PS. Mechanisms of viral membrane fusion and its inhibition. *Annu Rev Biochem.* 2001; 70:777–810. [PubMed: 11395423]
105. Skehel JJ, Wiley DC. Receptor binding and membrane fusion in virus entry: the influenza hemagglutinin. *Annu Rev Biochem.* 2000; 69:531–69. [PubMed: 10966468]
106. Klenk HD, Garten W. Host cell proteases controlling virus pathogenicity. *Trends Microbiol.* 1994; 2:39–43. [PubMed: 8162439]
107. Wilson IA, Skehel JJ, Wiley DC. Structure of the haemagglutinin membrane glycoprotein of influenza virus at 3 Å resolution. *Nature.* 1981; 289:366–73. [PubMed: 7464906]
108. Stein BS, Gowda SD, Lifson JD, Penhallow RC, Bensch KG, Engleman EG. pH-independent HIV entry into CD4-positive T cells via virus envelope fusion to the plasma membrane. *Cell.* 1987; 49:659–68. [PubMed: 3107838]
109. White J, Matlin K, Helenius A. Cell fusion by Semliki Forest, influenza, and vesicular stomatitis viruses. *J Cell Biol.* 1981; 89:674–79. [PubMed: 6265470]
110. Mothes W, Boerger AL, Narayan S, Cunningham JM, Young JA. Retroviral entry mediated by receptor priming and low pH triggering of an envelope glycoprotein. *Cell.* 2000; 103:679–89. [PubMed: 11106737]
111. Belouzard S, Millet JK, Licitra BN, Whittaker GR. Mechanisms of coronavirus cell entry mediated by the viral spike protein. *Viruses.* 2012; 4:1011–33. [PubMed: 22816037]
112. Heald-Sargent T, Gallagher T. Ready, set, fuse! The coronavirus spike protein and acquisition of fusion competence. *Viruses.* 2012; 4:557–80. [PubMed: 22590686]
113. Xu YH, Lou ZY, Liu YW, Pang H, Tien P, et al. Crystal structure of severe acute respiratory syndrome coronavirus spike protein fusion core. *J Biol Chem.* 2004; 279:49414–19. [PubMed: 15345712]
114. Lu L, Liu Q, Zhu Y, Chan KH, Qin L, et al. Structure-based discovery of Middle East respiratory syndrome coronavirus fusion inhibitor. *Nat Commun.* 2014; 5:3067. [PubMed: 24473083]
115. Zheng Q, Deng Y, Liu J, van der Hoek L, Berkhout B, Lu M. Core structure of S2 from the human coronavirus NL63 spike glycoprotein. *Biochemistry.* 2006; 45:15205–15. [PubMed: 17176042]
116. Xu Y, Liu Y, Lou Z, Qin L, Li X, et al. Structural basis for coronavirus-mediated membrane fusion. Crystal structure of mouse hepatitis virus spike protein fusion core. *J Biol Chem.* 2004; 279:30514–22. [PubMed: 15123674]
117. Duquerroy S, Vigouroux AN, Rottier PJM, Rey FA, Bosch BJ. Central ions and lateral asparagine/glutamine zippers stabilize the post-fusion hairpin conformation of the SARS coronavirus spike glycoprotein. *Virology.* 2005; 335:276–85. [PubMed: 15840526]
118. Gao J, Lu G, Qi J, Li Y, Wu Y, et al. Structure of the fusion core and inhibition of fusion by a heptad repeat peptide derived from the S protein of Middle East respiratory syndrome coronavirus. *J Virol.* 2013; 87:13134–40. [PubMed: 24067982]
119. Supekar VM, Bruckmann C, Ingallinella P, Bianchi E, Pessi A, Carfi A. Structure of a proteolytically resistant core from the severe acute respiratory syndrome coronavirus S2 fusion protein. *PNAS.* 2004; 101:17958–63. [PubMed: 15604146]
120. Millet JK, Whittaker GR. Host cell proteases: critical determinants of coronavirus tropism and pathogenesis. *Virus Res.* 2015; 202:120–34. [PubMed: 25445340]

121. Spaan W, Cavanagh D, Horzinek MC. Coronaviruses: structure and genome expression. *J Gen Virol.* 1988; 69:2939–52. [PubMed: 3058868]
122. Matsuyama S, Taguchi F. Receptor-induced conformational changes of murine coronavirus spike protein. *J Virol.* 2002; 76:11819–26. [PubMed: 12414924]
123. Zelus BD, Schickli JH, Blau DM, Weiss SR, Holmes KV. Conformational changes in the spike glycoprotein of murine coronavirus are induced at 37° C either by soluble murine CEACAM1 receptors or by pH 8. *J Virol.* 2003; 77:830–40. [PubMed: 12502799]
124. Qiu Z, Hingley ST, Simmons G, Yu C, Das Sarma J, et al. Endosomal proteolysis by cathepsins is necessary for murine coronavirus mouse hepatitis virus type 2 spike-mediated entry. *J Virol.* 2006; 80:5768–76. [PubMed: 16731916]
125. Eifart P, Ludwig K, Bottcher C, de Haan CA, Rottier PJ, et al. Role of endocytosis and low pH in murine hepatitis virus strain A59 cell entry. *J Virol.* 2007; 81:10758–68. [PubMed: 17626088]
126. Nakagaki K, Nakagaki K, Taguchi F. Receptor-independent spread of a highly neurotropic murine coronavirus JHMV strain from initially infected microglial cells in mixed neural cultures. *J Virol.* 2005; 79:6102–10. [PubMed: 15857995]
127. Gallagher TM, Buchmeier MJ, Perlman S. Cell receptor-independent infection by a neurotropic murine coronavirus. *Virology.* 1992; 191:517–22. [PubMed: 1413526]
128. Taguchi F, Matsuyama S, Saeki K. Difference in Bgp-independent fusion activity among mouse hepatitis viruses. *Arch Virol.* 1999; 144:2041–49. [PubMed: 10550676]
129. Krueger DK, Kelly SM, Lewicki DN, Ruffolo R, Gallagher TM. Variations in disparate regions of the murine coronavirus spike protein impact the initiation of membrane fusion. *J Virol.* 2001; 75:2792–802. [PubMed: 11222703]
130. Ontiveros E, Kim TS, Gallagher TM, Perlman S. Enhanced virulence mediated by the murine coronavirus, mouse hepatitis virus strain JHM, is associated with a glycine at residue 310 of the spike glycoprotein. *J Virol.* 2003; 77:10260–69. [PubMed: 12970410]
131. Miura TA, Travanty EA, Oko L, Bielefeldt-Ohmann H, Weiss SR, et al. The spike glycoprotein of murine coronavirus MHV-JHM mediates receptor-independent infection and spread in the central nervous systems of *Ceacam1a*<sup>-/-</sup> mice. *J Virol.* 2008; 82:755–63. [PubMed: 18003729]
132. Phillips JM, Weiss SR. Pathogenesis of neurotropic murine coronavirus is multifactorial. *Trends Pharmacol Sci.* 2011; 32:2–7. [PubMed: 21144598]
133. Song HC, Seo MY, Stadler K, Yoo BJ, Choo QL, et al. Synthesis and characterization of a native, oligomeric form of recombinant severe acute respiratory syndrome coronavirus spike glycoprotein. *J Virol.* 2004; 78:10328–35. [PubMed: 15367599]
134. Xiao X, Chakraborti S, Dimitrov AS, Gramatikoff K, Dimitrov DS. The SARS-CoV S glycoprotein: expression and functional characterization. *Biochem Biophys Res Commun.* 2003; 312:1159–64. [PubMed: 14651994]
135. Simmons G, Gosalia DN, Rennekamp AJ, Reeves JD, Diamond SL, Bates P. Inhibitors of cathepsin L prevent severe acute respiratory syndrome coronavirus entry. *PNAS.* 2005; 102:11876–81. [PubMed: 16081529]
136. Simmons G, Reeves JD, Rennekamp AJ, Amberg SM, Piefer AJ, Bates P. Characterization of severe acute respiratory syndrome-associated coronavirus (SARS-CoV) spike glycoprotein-mediated viral entry. *PNAS.* 2004; 101:4240–45. [PubMed: 15010527]
137. Huang IC, Bosch BJ, Li F, Li WH, Lee KH, et al. SARS coronavirus, but not human coronavirus NL63, utilizes cathepsin L to infect ACE2-expressing cells. *J Biol Chem.* 2006; 281:3198–203. [PubMed: 16339146]
138. Glowacka I, Bertram S, Muller MA, Allen P, Soilleux E, et al. Evidence that TMPRSS2 activates the severe acute respiratory syndrome coronavirus spike protein for membrane fusion and reduces viral control by the humoral immune response. *J Virol.* 2011; 85:4122–34. [PubMed: 21325420]
139. Bertram S, Glowacka I, Muller MA, Lavender H, Gnirss K, et al. Cleavage and activation of the severe acute respiratory syndrome coronavirus spike protein by human airway trypsin-like protease. *J Virol.* 2011; 85:13363–72. [PubMed: 21994442]

140. Shulla A, Heald-Sargent T, Subramanya G, Zhao J, Perlman S, Gallagher T. A transmembrane serine protease is linked to the severe acute respiratory syndrome coronavirus receptor and activates virus entry. *J Virol*. 2011; 85:873–82. [PubMed: 21068237]
141. Matsuyama S, Ujike M, Morikawa S, Tashiro M, Taguchi F. Protease-mediated enhancement of severe acute respiratory syndrome coronavirus infection. *PNAS*. 2005; 102:12543–47. [PubMed: 16116101]
142. Kam YW, Okumura Y, Kido H, Ng LF, Bruzzone R, Altmeyer R. Cleavage of the SARS coronavirus spike glycoprotein by airway proteases enhances virus entry into human bronchial epithelial cells in vitro. *PLOS ONE*. 2009; 4:e7870. [PubMed: 19924243]
143. Belouzard S, Chu VC, Whittaker GR. Activation of the SARS coronavirus spike protein via sequential proteolytic cleavage at two distinct sites. *PNAS*. 2009; 106:5871–76. [PubMed: 19321428]
144. Belouzard S, Madu I, Whittaker GR. Elastase-mediated activation of the severe acute respiratory syndrome coronavirus spike protein at discrete sites within the S2 domain. *J Biol Chem*. 2010; 285:22758–63. [PubMed: 20507992]
145. Beniac DR, de Varennes SL, Andonov A, He R, Booth TF. Conformational reorganization of the SARS coronavirus spike following receptor binding: implications for membrane fusion. *PLOS ONE*. 2007; 2:e1082. [PubMed: 17957264]
146. Simmons G, Zmora P, Gierer S, Heurich A, Pohlmann S. Proteolytic activation of the SARS-coronavirus spike protein: cutting enzymes at the cutting edge of antiviral research. *Antivir Res*. 2013; 100:605–14. [PubMed: 24121034]
147. Millet JK, Whittaker GR. Host cell entry of Middle East respiratory syndrome coronavirus after two-step, furin-mediated activation of the spike protein. *PNAS*. 2014; 111:15214–19. [PubMed: 25288733]
148. Qian Z, Dominguez SR, Holmes KV. Role of the spike glycoprotein of human Middle East respiratory syndrome coronavirus (MERS-CoV) in virus entry and syncytia formation. *PLOS ONE*. 2013; 8:e76469. [PubMed: 24098509]
149. Shirato K, Kawase M, Matsuyama S. Middle East respiratory syndrome coronavirus infection mediated by the transmembrane serine protease TMPRSS2. *J Virol*. 2013; 87:12552–61. [PubMed: 24027332]
150. Gierer S, Bertram S, Kaup F, Wrensch F, Heurich A, et al. The spike protein of the emerging  $\beta$ -coronavirus EMC uses a novel coronavirus receptor for entry, can be activated by TMPRSS2, and is targeted by neutralizing antibodies. *J Virol*. 2014; 87:5502–11.
151. Gierer S, Muller MA, Heurich A, Ritz D, Springstein BL, et al. Inhibition of proprotein convertases abrogates processing of the Middle Eastern respiratory syndrome coronavirus spike protein in infected cells but does not reduce viral infectivity. *J Infect Dis*. 2015; 211:889–97. [PubMed: 25057042]
152. Yang Y, Liu C, Du L, Jiang S, Shi Z, et al. Two mutations were critical for bat-to-human transmission of Middle East respiratory syndrome coronavirus. *J Virol*. 2015; 89:9119–23. [PubMed: 26063432]

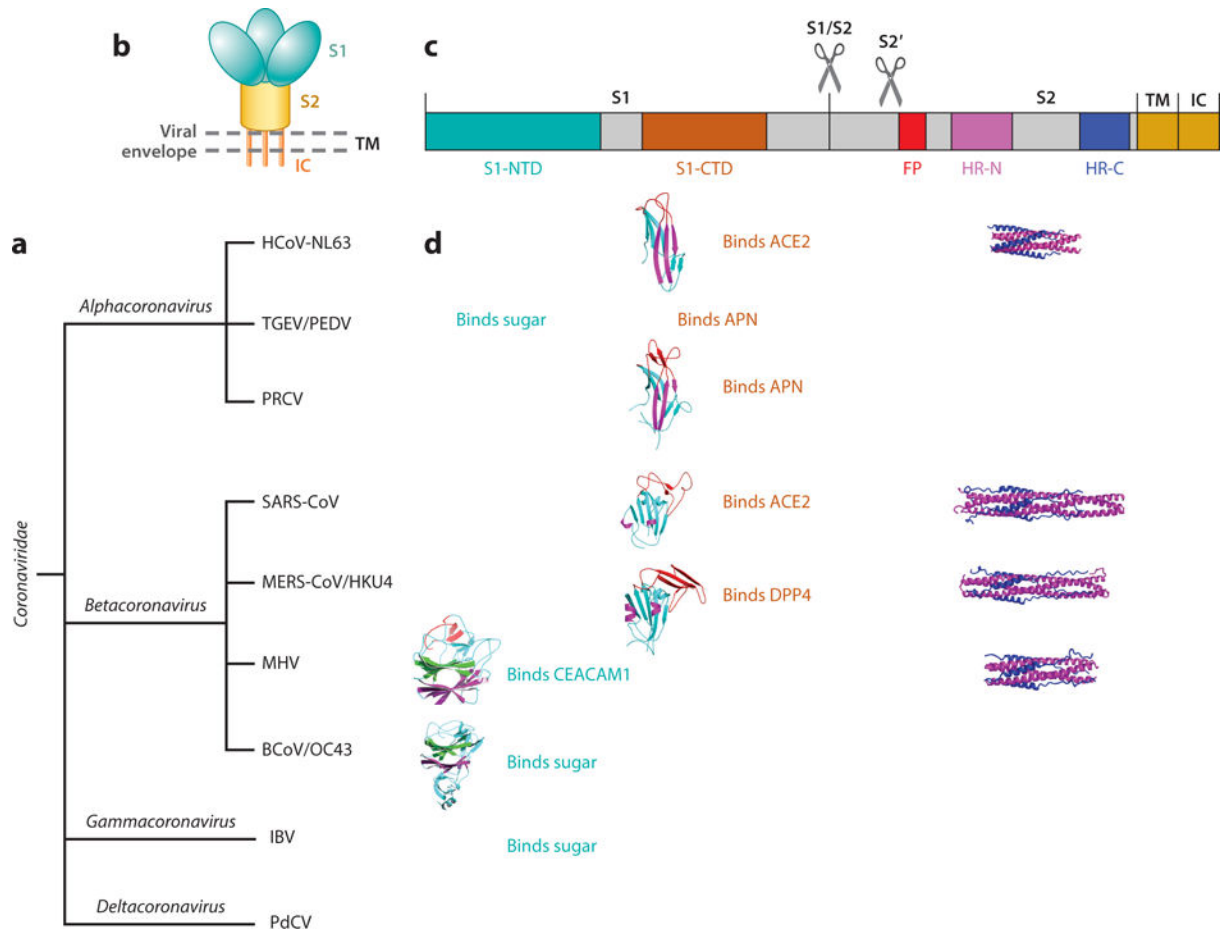


**Figure 1.**

Introduction to coronaviruses and their spike proteins. (a) Classification of coronaviruses. Representative coronaviruses in each genus are human coronavirus NL63 (HCoV-NL63), porcine transmissible gastroenteritis coronavirus (TGEV), porcine epidemic diarrhea coronavirus (PEDV), and porcine respiratory coronavirus (PRCV) in the genus *Alphacoronavirus*; severe acute respiratory syndrome coronavirus (SARS-CoV), Middle East respiratory syndrome coronavirus (MERS-CoV), bat coronavirus HKU4, mouse hepatitis coronavirus (MHV), bovine coronavirus (BCoV), and human coronavirus OC43 in the genus *Betacoronavirus*; avian infectious bronchitis coronavirus (IBV) in the genus *Gammacoronavirus*; and porcine deltacoronavirus (PdCV) in the genus *Deltacoronavirus*. (b) Schematic of the overall structure of prefusion coronavirus spikes. Shown are the receptor-binding subunit S1, the membrane-fusion subunit S2, the transmembrane anchor (TM), the intracellular tail (IC), and the viral envelope. (c) Schematic of the domain structure of coronavirus spikes, including the S1 N-terminal domain (S1-NTD), the S1 C-terminal domain (S1-CTD), the fusion peptide (FP), and heptad repeat regions N and C (HR-N and HR-C). Scissors indicate two proteolysis sites in coronavirus spikes. (d) Summary of the structures and functions of coronavirus spikes. Host receptors recognized by either of the S1 domains are angiotensin-converting enzyme 2 (ACE2), aminopeptidase N (APN), dipeptidyl peptidase 4 (DPP4), carcinoembryonic antigen-related cell adhesion molecule 1 (CEACAM1), and sugar. The available crystal structures of S1 domains and S2

HRs are shown. Their PDB IDs are 3KBH for HCoV-NL63 S1-CTD, 4F5C for PRCV S1-CTD, 2AJF for SARS-CoV S1-CTD, 4KR0 for MERS-CoV S1-CTD, 3R4D for MHV S1-NTD, 4H14 for BCoV S1-NTD, 2IEQ for HCoV-NL63 HRs, 1WYY for SARS-CoV HRs, 4NJL for MERS-CoV HRs, and 1WDF for MHV HRs.

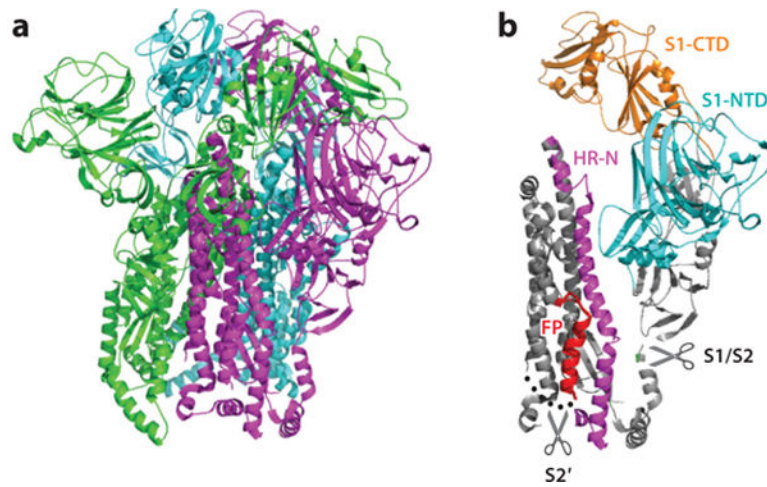


**Figure 2.**

Cryo-electron microscopy structures of prefusion trimeric coronavirus spikes. (a) Trimeric mouse hepatitis coronavirus (MHV) spike (PDB ID: 3JCL) (16). Three monomers are shown (*magenta*, *cyan*, and *green*). (b) One monomer from the trimeric MHV spike. The important functional elements of the spike [the S1 N-terminal domain (S1-NTD), the S1 C-terminal domain (S1-CTD), the fusion peptide (FP), and the heptad repeat (HR-N)] are colored in the same way as in Figure 1c. The dotted curve indicates a disordered loop. Scissors indicate two critical proteolysis sites.

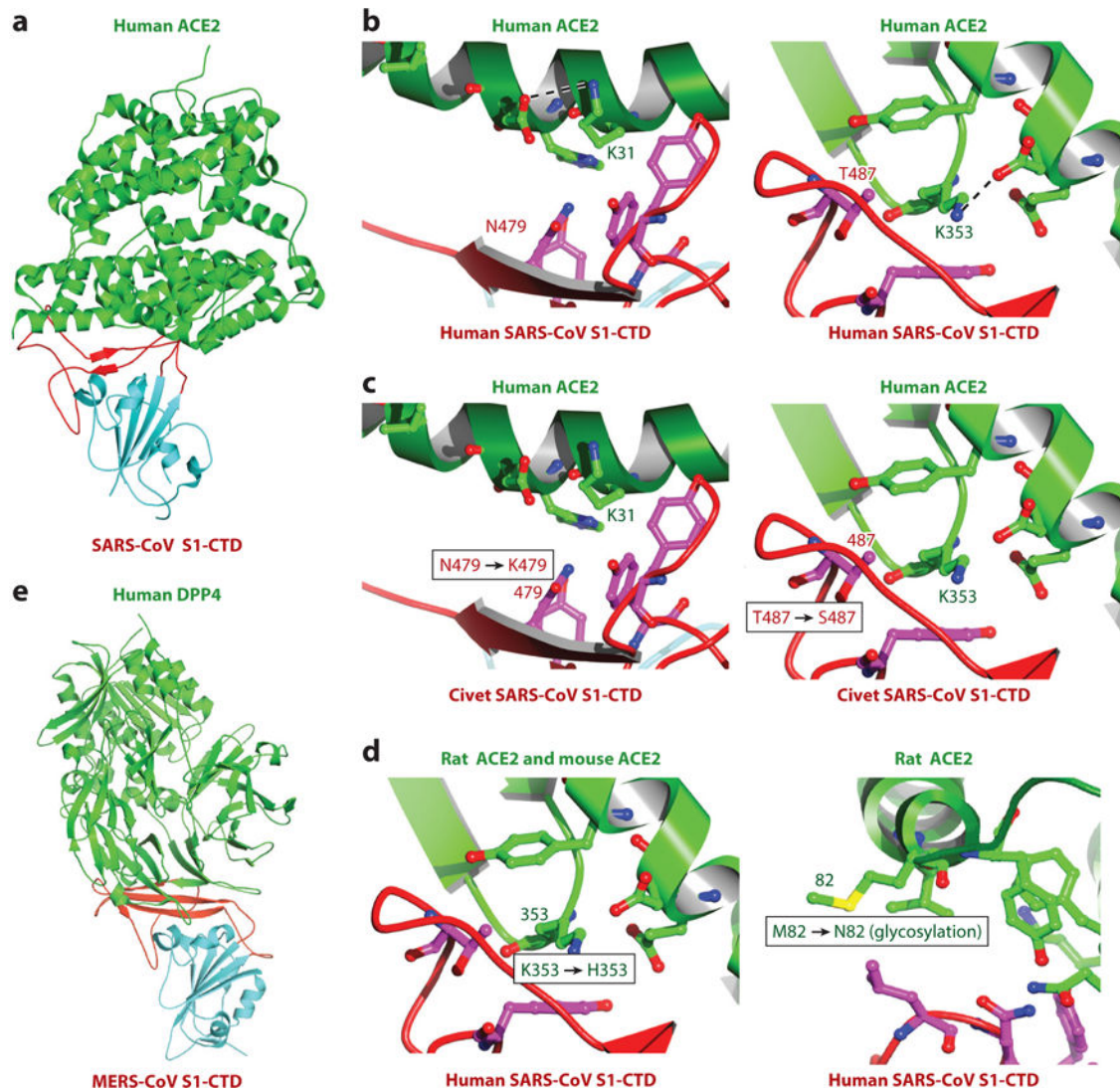


**Figure 3.**

Crystal structures of betacoronavirus S1 C-terminal domains (S1-CTDs). (a) Structure of severe acute respiratory syndrome coronavirus (SARS-CoV) S1-CTD complexed with human ACE2 (PDB ID: 2AJF) (52). Shown are the core structure of S1-CTD (*cyan*), the receptor-binding motif (*red*), and ACE2 (*green*). (b) Interface between human SARS-CoV S1-CTD and human ACE2, showing two virus-binding hot spots on human ACE2. Dashed lines indicate salt bridges. (c) Interface between palm civet SARS-CoV S1-CTD and human ACE2. Critical residue changes from human to civet SARS-CoV strains are labeled. (d) Interface between human SARS-CoV S1-CTD and rat or mouse ACE2. Critical residue changes from human to rat or mouse ACE2 are labeled. (e) Structure of Middle East respiratory syndrome coronavirus (MERS-CoV) S1-CTD complexed with human DPP4 (PDB ID: 4KR0) (69).

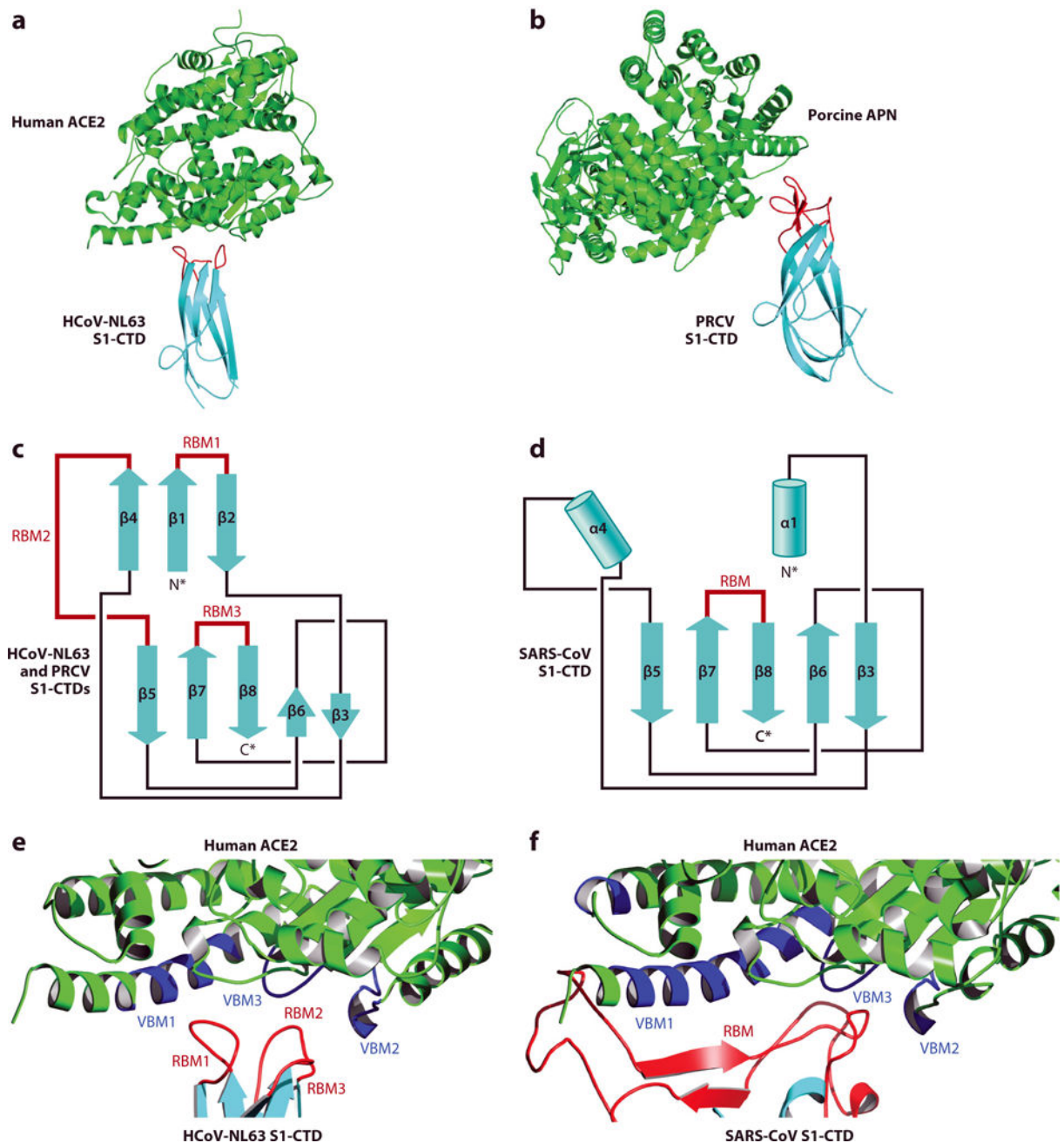


**Figure 4.**

Crystal structures of alphacoronavirus S1 C-terminal domains (S1-CTDs). (a) Structure of human coronavirus NL63 (HCoV-NL63) S1-CTD complexed with human ACE2 (PDB ID: 4KBH) (83). (b) Structure of porcine respiratory coronavirus (PRCV) S1-CTD complexed with porcine APN (PDB ID: 4F5C) (84). (c) Structural topology of alphacoronavirus S1-CTDs.  $\beta$ -Strands are shown as arrows. (d) Structural topology of betacoronavirus S1-CTDs.  $\alpha$ -Helices are shown as cylinders. All of the secondary structural elements in panels c and d are connected in the same order, even though strands  $\beta_4$ ,  $\beta_1$ , and  $\beta_2$  in panel c become helices  $\alpha_4$ ,  $\alpha_1$ , and a loop, respectively, in panel d. (e) Interface between HCoV-NL63 S1-

CTD and human ACE2. Virus-binding motifs (VBM) on ACE2 are shown in blue. Receptor-binding motifs (RBM) on S1-CTD are shown in red. (f) Interface between SARS-CoV S1-CTD and human ACE2.

Author Manuscript

Author Manuscript

Author Manuscript

Author Manuscript

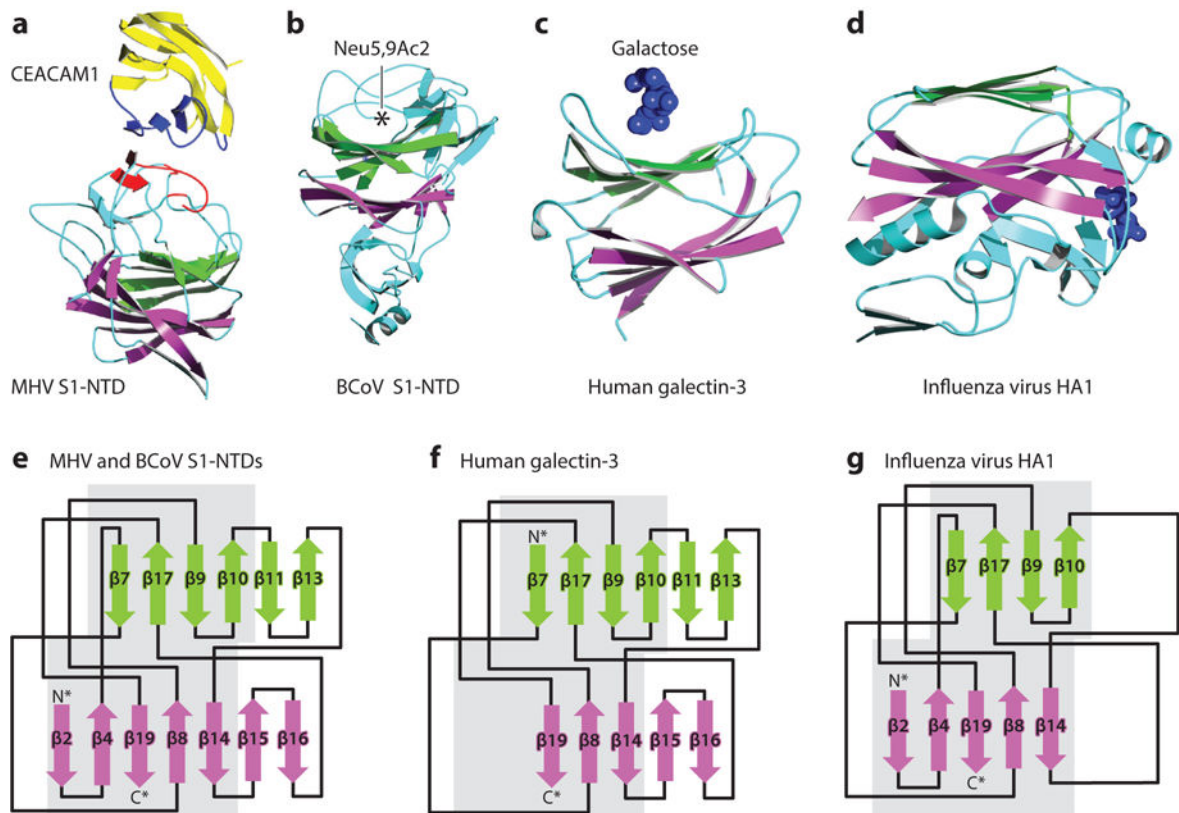


**Figure 5.**

Crystal structures of betacoronavirus S1 N-terminal domains (S1-NTDs). (a) Structure of mouse hepatitis coronavirus (MHV) S1-NTD complexed with murine CEACAM1 (PDB ID: 3R4D) (88). The core structure of MHV S1-NTD is shown in magenta and green, the receptor-binding motifs in red, and the rest in cyan. The N-terminal immunoglobulin domain of CEACAM1 is shown in yellow and virus-binding motifs in blue. (b) Structure of bovine coronavirus (BCoV) S1-NTD (PDB ID: 4H14) (43). The asterisk indicates the binding site for sugar receptor Neu5,9Ac2. (c) Structure of human galectin-3 complexed with galactose (PDB ID: 1A3K). Sugar receptor is shown in blue. (d) Structure of influenza virus HA1 (PDB ID: 1J5O). Sugar receptor is shown in blue. (e–g) Structural topologies of (e) betacoronavirus S1-NTDs, (f) human galectins, and (g) influenza virus HA1.

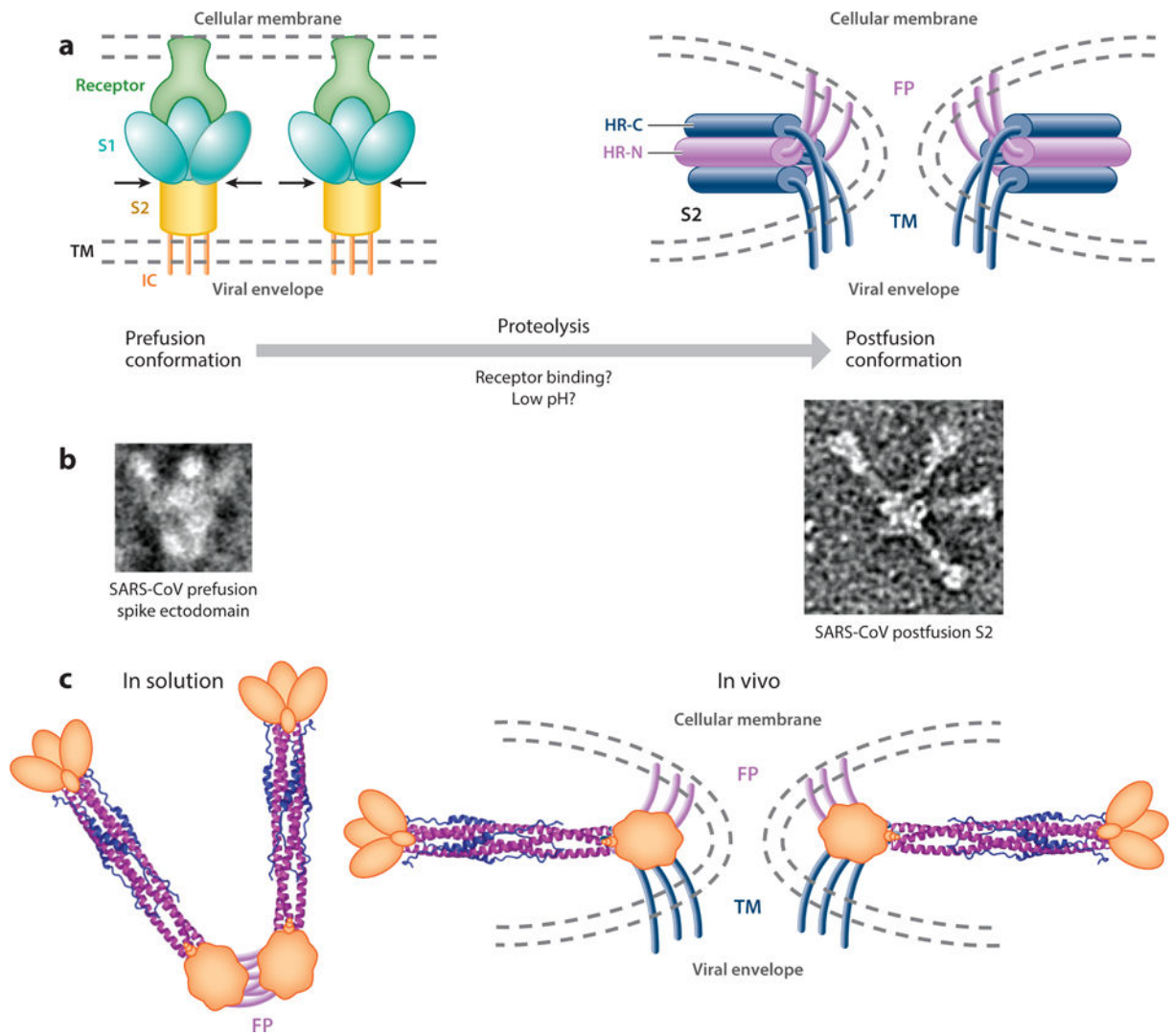


**Figure 6.** Structural mechanism for membrane fusion by coronavirus spikes. (a) Structural mechanism for membrane fusion by class I viral membrane fusion proteins. Schematics of these proteins in both prefusion and postfusion conformations are shown. (b) Negative-stain electron microscopy images of SARS-CoV spike in both prefusion and postfusion conformations are shown (18). (c) Schematics of SARS-CoV postfusion S2 in solution (*left*) and in vivo (*right*). Abbreviations: FP, fusion peptide; HR-N, heptad repeat region N; HR-C, heptad repeat region C; IC, intracellular tail; SARS-CoV, severe acute respiratory syndrome coronavirus; TM, transmembrane anchor.

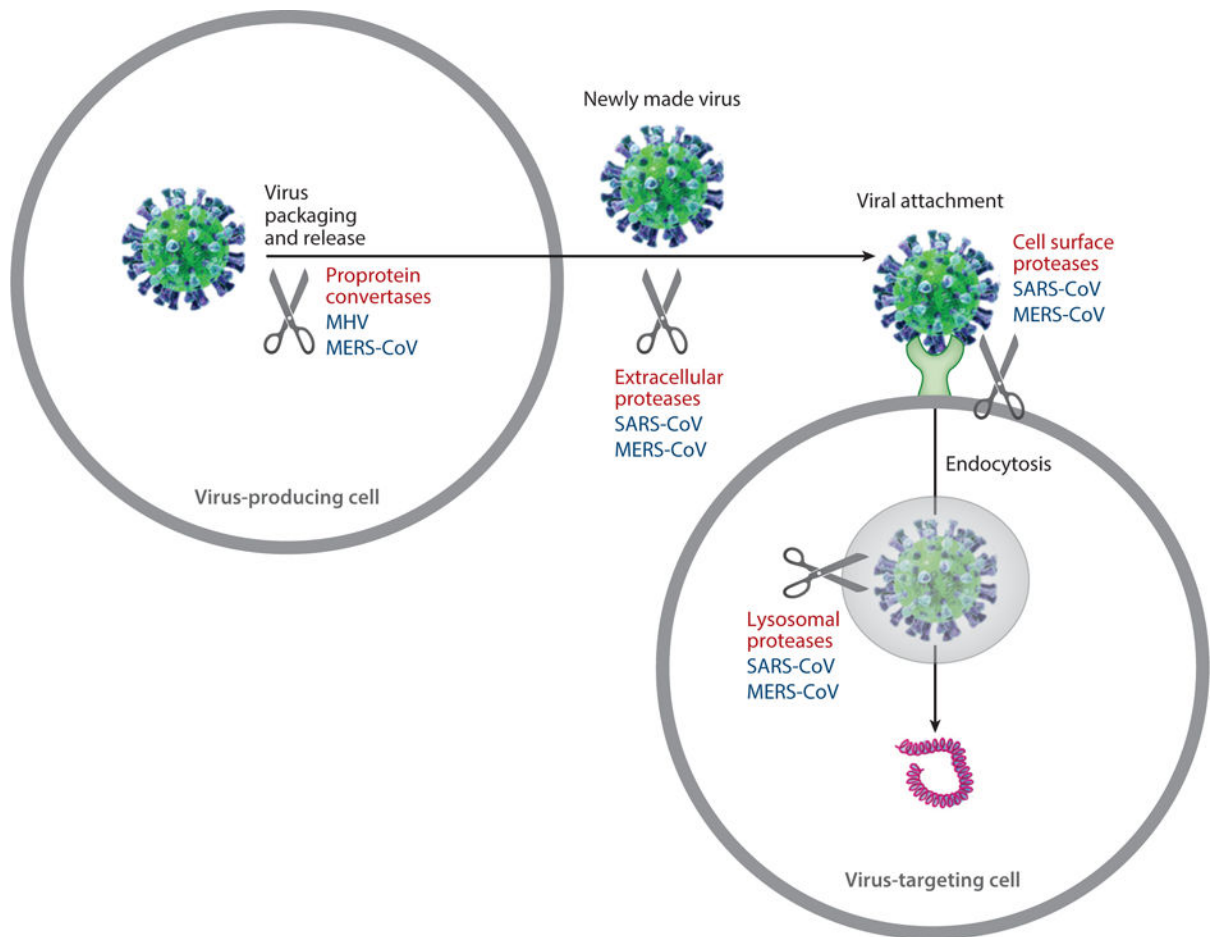


**Figure 7.**

Triggers for coronavirus spikes to fuse membranes. Scissors indicate potential spike-processing host proteases. Shown are virus particles (*green spheres*), virus surface spikes (*blue protrusions*), viral genome (*magenta coils*), cells (*large gray circles*), endosome/lysosome (*small shaded gray circle*), and receptor (*light green base on cell surface*). Spike-processing host proteases are labeled for representative coronaviruses: Middle East respiratory syndrome coronavirus (MERS-CoV), mouse hepatitis coronavirus (MHV), and severe acute respiratory syndrome coronavirus (SARS-CoV).

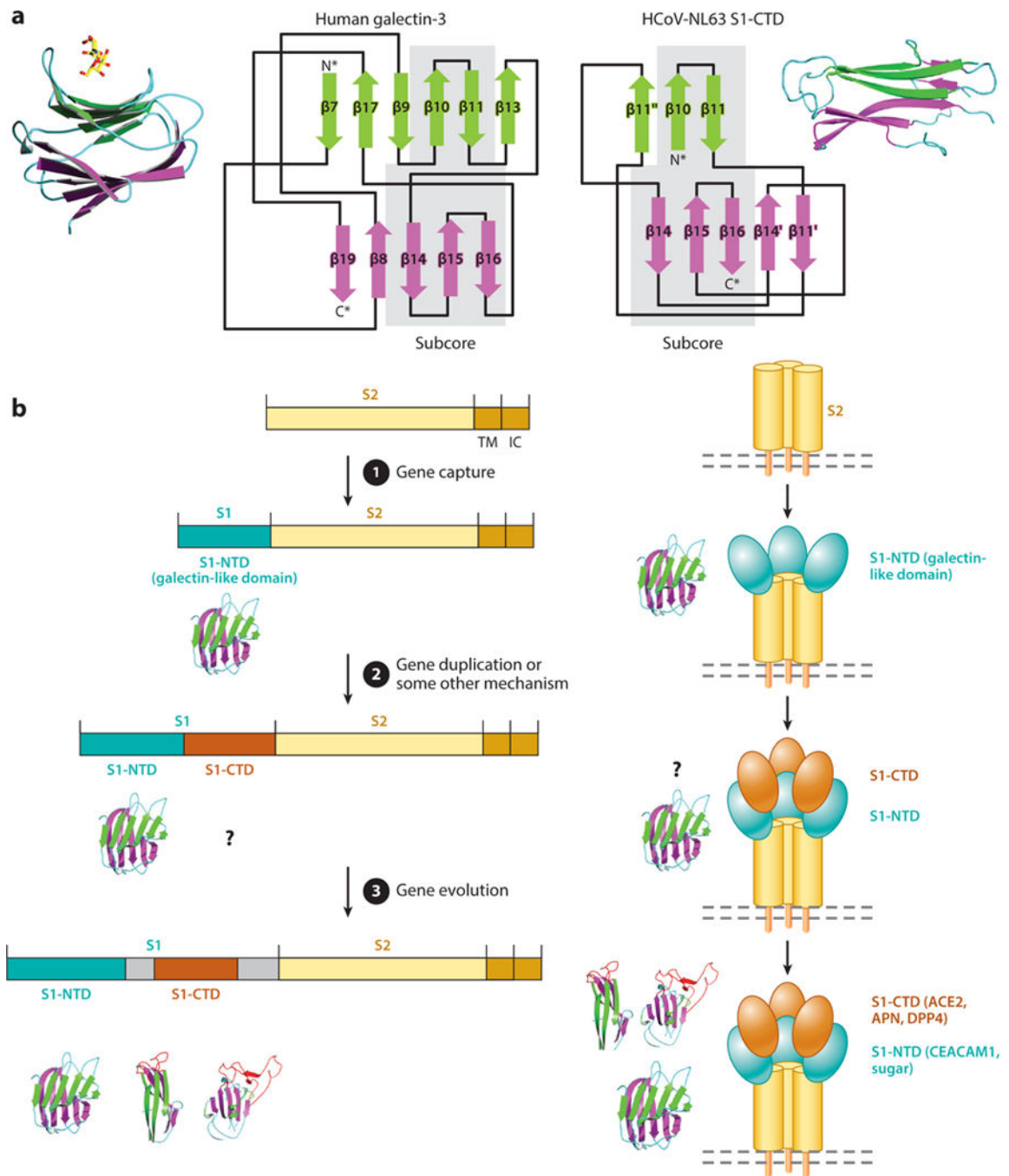


**Figure 8.** Evolution of coronavirus spikes. (a) Structural comparison between human galectins and alphacoronavirus HCoV-NL63 S1-CTD. Both the crystal structures and structural topologies of the two proteins are shown. Common subcore structures in the two proteins are highlighted with gray shading. (b) Hypothesized evolution of coronavirus spike proteins. Abbreviations: HCoV-NL63, human coronavirus NL63; IC, intracellular tail; S1-CTD, S1 C-terminal domain; S1-NTD, S1 N-terminal domain; TM, transmembrane anchor.